Molecular Biology of the Cell
Vol. 9, 2785–2802, October 1998

Fibroblast Growth Factor (FGF) Soluble Receptor 1 Acts as a Natural Inhibitor of FGF2 Neurotrophic Activity during Retinal Degeneration

Xavier Guillonneau,* Fabienne Régnier-Ricard,* Olivier Laplace,* Laurent Jonet,* Marijke Bryckaert,† Yves Courtois,* and Frédéric Mascarelli*‡

*Développement, Vieillissement et Pathologie de la Rétine, Institut National de la Santé et de la Recherche Médicale U450, Affiliée Centre National de la Recherche Scientifique, Association Claude Bernard, 75016 Paris, France; and †Institut National de la Santé et de la Recherche Médicale U248, Hôpital Lariboisière, IFR Circulation, 75010 Paris, France

Submitted October 31, 1997; Accepted June 25, 1998
Monitoring Editor: Joseph Schlessinger

Fibroblast growth factors (FGF) 1 and 2 and their tyrosine kinase receptor (FGFR) are present throughout the adult retina. FGFs are potential mitogens, but adult retinal cells are maintained in a nonproliferative state unless the retina is damaged. Our work aims to find a modulator of FGF signaling in normal and pathological retina. We identified and sequenced a truncated FGFR1 form from rat retina generated by the use of selective polyadenylation sites. This 70-kDa form of soluble extracellular FGFR1 (SR1) was distributed mainly localized in the inner nuclear layer of the retina, whereas the full-length FGFR1 form was detected in the retinal Muller glial cells. FGF2 and FGFR1 mRNA levels greatly increased in light-induced retinal degeneration. FGFR1 was detected in the radial fibers of activated retinal Muller glial cells. In contrast, SR1 mRNA synthesis followed a biphasic pattern of down- and up-regulation, and anti-SR1 staining was intense in retinal pigmented epithelial cells. The synthesis of SR1 and FGFR1 specifically and independently regulated in normal and degenerating retina suggests that changes in the proportion of various FGFR forms may control the bioavailability of FGFs and thus their potential as neurotrophic factors. This was demonstrated in vivo during retinal degeneration when recombinant SR1 inhibited the neurotrophic activity of exogenous FGF2 and increased damaging effects of light by inhibiting endogenous FGF. This study highlights the significance of the generation of SR1 in normal and pathological conditions.

INTRODUCTION

Fibroblast growth factors (FGFs) are a family of at least 15 structurally related mitogenic factors that exert their biological effects on cells of various mesenchymal and neuroectodermal origins (reviewed in Courlier *et al.*, 1997). Acidic FGF (FGF1) and basic FGF (FGF2), the prototype members of this family, are abundant in nervous tissue and have been purified from the retina (Baird *et al.*, 1984; Courty *et al.*, 1985). FGFs are implicated in regulating retinal cellular events, including cell proliferation, migration, differentiation, and survival (Barnstable, 1991). FGF1 and FGF2 interact with tyrosine kinase receptors (FGFRs) (Ruta *et al.*, 1988; Lee *et al.*, 1989; Craig *et al.*, 1990; Jaye *et al.*, 1992) and low-affinity binding sites, identified as heparan sulfate proteoglycans (Moscatelli, 1987; Yayon *et al.*, 1991; Mascarelli *et al.*, 1993; Wiedlocha *et al.*, 1994). Four genes encode the four forms of FGFR1–4, which have a common structure composed of two or three extracellular immunoglobulin (Ig)-like loops (IgI–IgIII) and one intracellular tyrosine kinase

‡ Corresponding author.

domain. For FGFR1–3, alternative splicing of the exon encoding the extracellular region produces multiple receptor forms (Johnson *et al.*, 1991; Givol and Yayon, 1992). The genomic organization of the third Ig-like loop leads to three receptor variants. Two membrane-spanning forms are produced by alternative splicing of two exons (IIIb and IIIc) encoding the second half of loop III, whereas a selective polyadenylation site preceding exons IIIb and IIIc is used to produce a soluble form of FGFR1 (IIIa). In humans and mice, the mRNA transcript of the IgIIIa splice variant of FGFR1 encodes a protein that potentially has no hydrophobic membrane-spanning domain and may therefore be a secreted form of the receptor (SR) (Werner *et al.*, 1992).

Little is known about the synthesis and functions of the truncated FGFR forms in vivo. Deletion of the transmembrane domain and most of the kinase domain (Yamaguchi *et al.*, 1994) and deletion of the IgII domain (Deng *et al.*, 1994) have demonstrated that the FGFR1 signaling pathway regulates early embryonic cell proliferation and mediates mesodermal patterning during gastrulation and somitogenesis. Significant changes in the phenotypes of the homozygotes for the deleted FGFR1 gene have been attributed to the synthesis of truncated FGFR gene products competing for ligand binding with the full-length FGFRs. It has also been suggested that differential expression of all FGFR genes and tissue-specific alternative splicing of FGFR mRNA may account for differences in their function (Partanen *et al.*, 1992; Werner *et al.*, 1992; Wang *et al.*, 1994). Thus, the effects of FGFs depend on the synthesis of temporally and spatially regulated variants of their receptors (Beck *et al.*, 1994; Johnston *et al.*, 1995). Robinson *et al.* (1995b), using mice transformed with the coding sequence of a secreted form of FGF1, suggested that resistance of some cells to the differentiation activity of FGF1 was due to FGF-inhibiting proteins. These plasma proteins entering the vitreous via permeable blood vessels and inhibiting the FGF1 signals may be truncated FGFR. This notion was supported by the synthesis of truncated FGFR1 in transgenic mice resulting in defective lens development (Robinson *et al.*, 1995a). Three FGF-binding proteins (FGF-BPs) comprising the extracellular domains of FGFR1 were detected in serum (Hanneken *et al.*, 1994) and in the vitreous (Hanneken and Baird, 1995) by immunochemistry. Truncated forms of the full-length FGF receptor were also detected in the basement membrane of retinal vascular endothelial cells (Hanneken *et al.*, 1995). The natural production of these extracellular domains of FGFR1 may result from several mechanisms: 1) a transcriptional event involving an alternative exon encoding soluble truncated receptor 1 (SR1) (Werner *et al.*, 1992), and 2) posttranslational modification producing FGF-BPs, which are forms of the extracellular domain of FGFR1.

To determine whether the transcriptional mechanism to generate SR1 occurs in vivo, we used a PCR-based approach to amplify a rat retina cDNA encompassing the first half of the IgII loop to the second half of the SR1-specific IgIII loop. We show that, in the retina, differential splicing of the exon encoding the extracellular region of the FGFR1 gene generates both the soluble receptor SR1 (IgIIIa) and the full-length tyrosine kinase receptor (IgIIIc) variants. SR1 bound to FGF2. Human recombinant SR1 and a polyclonal antibody directed against the rat IgIIIa-like loop of SR1 were prepared to investigate SR1 regulation. Analysis of the expression patterns of SR1 and FGFR1 genes during FGF2 overproduction in experimentally induced retina degeneration and the in vivo inhibitory effect of SR1 on the FGF2-induced photoreceptor rescue strongly suggests that SR1 is involved in the regulation of FGF activity in normal and degenerating retina.

MATERIALS AND METHODS

RNA Extraction, Reverse Transcription, and Sequencing

Total RNA was isolated by the guanidium-isothiocyanate method (Chirgwin *et al.*, 1978). Total RNA was used as template to produce cDNA using Moloney murine leukemia virus reverse transcriptase (Life Technologies, Ceigy Pontoise, France) and random hexanucleotide primers. Total RNA (1 μg) was heated with 70 μM hexamer at 65°C for 5 min, rapidly chilled on ice for 5 min and then added to the retro-transcription (RT) reaction mix [50 M Tris-HCl, pH 8.3, 75 mM KCl, 4 mM $MgCl_2$, 0.5 mM dNTPs, 5 mM DTT, 10 U of RNA guard [Pharmacia, Piscataway, NJ], and 200 U of Moloney murine leukemia virus reverse transcriptase). The mixture was incubated for 10 min at 21°C, then for 90 min at 42°C, and finally for 5 min at 94°C. The RT reaction mixtures were then rapidly chilled on ice and stored at −20°C until use.

cDNA was produced from Fisher rat by reverse transcription of 1 μg of total RNA extracted from either neural retina or retinal pigmented epithelial (RPE) cells. We amplified a 530-bp cDNA fragment encoding FGFR1 by PCR. Oligonucleotides were designed based on sequences from regions of high interspecies homology. The sense oligonucleotide (5′-AAC GGC AAG GAA TTC AAA CCG G-3′) was derived from exon 3, encoding the first part of loop two. The antisense oligonucleotide IAS (5′-CCC TCT GTT CCC AGT TCA CC-3′) was derived from the untranslated region of the mouse FGFR1 sequence. The purified PCR fragment was inserted into the pGEM-T vector (Promega, Lyon, France) according to the manufacturer's protocol. Three clones were selected for each tissue and sequenced in forward and reverse directions using the Thermosequenase fluorescent labeled primer cycle sequencing kit (Amersham, Les Ulis, France). For each clone, 1 μg of plasmid DNA was amplified over 30 cycles using the forward or reverse M13-fluorescent oligonucleotide. Sequences were analyzed with BaseImagIR version 2.2 software (LiCor, Lincoln, NE), and all three sequences were identical.

Preparation of Rabbit Polyclonal Anti-SR1 Antibody

A polyclonal antibody directed against the 13-amino-acid peptide (VILASFLASLLGR) from the carboxyl terminus encoded by the IgIIIa exon of soluble FGFR1 was produced. The peptide, conjugated to keyhole limpet hemocyanin in complete Freund's adjuvant,

was injected subcutaneously into two rabbits. A test bleed and a preimmuno bleed were performed. Antigen injection was repeated on day 14 after primary immunization and every 2 weeks thereafter. The 13-amino-acid peptide was used to check the specificity of the anti-SR1 antibody (by antigen peptide preadsorption).

An affinity-purified anti-FGFR1 polyclonal antibody was raised against a peptide sequence from the carboxyl terminus of full-length human FGFR1 (Santa Cruz Biotechnology, Santa Cruz, CA). The specificity of the anti-FGFR1 was previously verified (McDewitt *et al.*, 1997). This antibody did not cross-react with FGFR2, FGFR3, or FGFR4. A control peptide, Sc-121 P, was used to check the specificity of the anti-FGFR1 antibody. The sequence of this peptide is well conserved in rat, mouse, and human FGFR1.

Identification of FGF Soluble Receptors

Two methods were used to identify the various forms of FGFR1 in rat retina: cross-linking to ^{125}I-FGF2 immobilized on heparin-Sepharose columns and ^{125}I-FGF2 blotting. Neural retina from Fisher rats was extracted with 40 mM CHAPS in PBS containing 1 mM PMSF, 1 μg/ml leupeptin, 5 μg/ml pepstatin, 20 Kallikrein inhibitor units of aprotinin, and 1 μg/ml trypsin inhibitor according to a bovine FGFR purification protocol (Torriglia and Blanquet, 1992). CHAPS extract (equivalent amounts of protein in each lane) was loaded on a heparin-Sepharose column (0.2-ml volume, 0.6 $\times$ 0.5 cm) on which ^{125}I-FGF2 (10 ng; specific activity [SA], 10^5 cpm/ng) was immobilized. Receptors were cross-linked to the bound FGF2 using 0.3 mM disuccinimidyl suberate (DSS). The ^{125}I-FGF2–receptor complexes were eluted with 2 M NaCl (pH 7.4), and 4 vol of PBS were added to the column. Solubilized FGF receptor complexes were immunoprecipitated by adding 20 μl of anti-SR1 or anti-full-length FGF-R1 antibodies, with or without incubation with the cognate antigen peptide (to check antibody specificity) and incubated overnight at 4°C. Protein A-Sepharose (40 μl) was then added, and the suspension was incubated for 1 h at 4°C. Protein A–Sepharose was collected by centrifugation. In control experiments, CHAPS fractions were incubated with a 500-fold excess of unlabeled FGF2 before loading on the column. ^{125}I-FGF2-FGF receptor 1 complexes were analyzed by SDS-PAGE (10% acrylamide gel) and autoradiography.

Immunohistochemistry

Eyes were obtained from normal adult Fisher rats (3 months old). Unfixed eyes were bisected along the vertical meridian, their lenses were removed, and the eye hemispheres were prepared for frozen sections. Retina sections were saturated with 1% BSA and 1% normal goat serum in PBS and permeabilized in 0.1% Triton X-100 for 30 min. The sections were then incubated for 1 h at 20°C with various primary antibodies. Slides were rinsed, incubated with a secondary, biotinylated donkey anti-rabbit IgG (1:100, Amersham) for 1 h at 20°C, and then incubated with fluorescein isothiocyanate–labeled extravidin (1:100 dilution; Sigma, Saint Quentin Fallavier, France). Slides were washed six times for 5 min each in PBS after each incubation and then mounted in glycerol-PBS (1:1 vol/vol) and examined with a Leitz (Wetzlar, Germany) Aristoplan microscope equipped with epifluorescence illumination. Photographs were taken with Ilford (Paramus, NJ) HP5 film (400 ASA). Various control experiments were performed to check the specificity of the anti-SR1, anti-FGFR1, anti-FGF1, and anti-FGF2 staining: 1) the primary antibody was omitted; 2) preimmune serum was used instead of primary antibody; 3) antibodies were blocked by incubation of the serum or the antibody with the cognate antigen peptides (40–100 μg/ml); and 4) identical incubations were performed with an equal concentration of nonantigen peptide. At least four adult rats were used, means of 10–20 sections per rat were stained with each antibody.

Sections were incubated with anti-glial fibrillary acidic protein (GFAP) antibody (1:100), anti-Von Willebrandt factor antibody (1:100, Dako, Trappes, France), anti-neurofilament (68 kDa) monoclonal antibody (1:400; Sigma, St. Louis, MO), and anti-synaptophysin antibody (1:100; Boehringer Mannheim, Meylan, France).

Recombinant SR1

The gene encoding the extracellular domain of the human FGF receptor type 1 (hrSR1) was kindly provided by Dr. P Caccia (Farmitalia Carlo Erba, Neviano, Italy) and was expressed in *Escherichia coli*. The gene product was purified to homogeneity as previously described (Bergonzoni *et al.*, 1992). Recombinant SR1 activity, the activity of control preparations from control bacterial extracts, and the purity of SR1 have already been characterized (Bergonzoni *et al.*, 1992; Caccia *et al.*, 1993). The amino acid sequence of human recombinant SR1 is 92% identical to that of rat SR1. The effects of purified hrSR1 on FGF-induced cell proliferation, FGF binding to FGFR1, and on ERK2 activation were not the result of contamination with bacterial agents because immunoprecipitation of the hrSR1 preparation with two blocking anti-FGFR extracellular domain antibodies (anti-chicken FGF receptor, Upstate Biotechnology, Lake Placid, NY [Lee *et al.*, 1989]; and mouse anti-bovine FGF receptor, Chemicon International, Temecula, CA [Wenkateswaren *et al.*, 1992]) completely abolished the inhibitory effects of hrSR1. This demonstrated the specificity and purity of the recombinant protein.

Mitogenic Assay

The mitogenic assay was performed as previously described (Mascarelli *et al.*, 1992). Monolayers of quiescent RPE cells were preincubated in DMEM without serum with various concentrations of recombinant SR1 at 37°C for 1 h. FGF1 (10 ng/ml) or FGF2 (10 ng/ml) was then added, and the cells were incubated at 37°C for 24 h. Mitogenic activity was measured by the incorporation of [^{3}H]thymidine (SA = 0.92 TBq/nmol) over the last 4 h of incubation with growth factor. A dose–response curve of activity was produced for each sample with each experiment performed at least three times.

Radioreceptor Assay and Cross-Linking Experiment

The radioreceptor assay was performed as previously described (Mascarelli *et al.*, 1989). Confluent RPE cells were incubated for 2 h at 4°C with various concentrations of recombinant SR1 and 5 ng/ml ^{125}I-FGF1 (SA = 5×10^4 cpm/ng) or ^{125}I-FGF2 (SA = 10^5 cpm/ng). Nonspecific binding of ^{125}I-FGF2 to RPE cells was determined using an excess (200-fold) of unlabeled FGF2. The cells were washed twice with 0.5 ml of PBS and twice with 0.5 ml of PBS containing 2 M NaCl as previously described (Moscatelli 1987) to discriminate between FGF high-affinity tyrosine kinase and low-affinity binding sites related to heparan sulfate proteoglycans. ^{125}I-FGF bound to high-affinity receptors was determined by quantifying the radioactivity in the cell lysate obtained with 0.1% Triton X-100 in PBS (pH 7.4), and the amount of ^{125}I-FGF bound to low-affinity binding sites was determined by quantifying radioactivity in the 2 M NaCl washes. All experiments were performed in triplicate.

Confluent RPE cells were incubated with 5 ng/ml ^{125}I-FGF1 or ^{125}I-FGF2 for 2 h at 4°C with or without 700 ng/ml SR1. In control experiments, a 200-fold excess of unlabeled FGF1 or FGF2 was also added. ^{125}I-FGF was cross-linked to FGFR1 at room temperature for 15 min using DSS, as previously described (Guillonneau *et al.*, 1996). Cross-linked receptors were separated by SDS-PAGE (7% acrylamide gel). The gels were then subjected to autoradiography.

Western Blot Analysis

Confluent RPE cells were transferred to DMEM without serum and cultured for a further 48 h. FGF2 (10 ng/ml) was added for various times in the presence of 700 ng/ml hrSR1 or in its absence. The cells were washed twice with PBS and lysed in 50 mM Tris-HCl (pH 7.4), 100 mM NaCl, 50 mM NaF, 5 mM EDTA, 40 mM β-glycerophosphate, 200 mM Na_3VO_4, 1 μg/ml leupeptin, 1 μM pepstatin, and 1%

Triton X-100. Cell lysates were subjected to SDS-PAGE (12% acrylamide gel), and the proteins were transferred onto nitrocellulose filters by electroblotting and probed with anti-ERK2 antibody (Santa Cruz Biotechnology). The primary antibody was detected using horseradish peroxidase–conjugated goat anti-rabbit IgG. Blots were then incubated with sheep anti-mouse IgG conjugated with horseradish peroxidase at a dilution of 1/5000. ECL substrates were used to detect positive bands according to the manufacturer's instructions (Amersham).

Light-induced Retinal Damage in Rats and Factor Injection

Retinal degeneration induced by light and checks on the degree of degeneration were performed as previously described (Goureau *et al.*, 1993). All procedures involving rats conformed to Association for Research in Vision and Ophthalmology resolution of the use of animals in research and to the guidelines of the Institut National de la Santé et de la Recherche Médicale Committee on Animal Research. Eight-week-old IOPS Fisher male rats (Iffa Credo, L'Arbreste, France) were kept in an environment with a daily dark cycle (12 h on, 12 h off) at a cage illumination of <20 foot candles for at least 4 d. They were then exposed to constant light, for 1–9 d, at an illumination level of 90 foot candles provided by two 20 W white fluorescent bulbs suspended 20 cm above the bottom of transparent polycarbonate cages.

To investigate the in vivo effects of SR1 on the FGF2-induced photoreceptor protection during constant illumination, 250 ng of FGF2 in the presence or absence of an 80-fold excess of SR1 (20 μg) were injected intravitreally 2 d before light exposure. The injections were made with the insertion of a fine glass micropipette (tip diameter, ~50 μm) instead of a 26 or 32 gauge injection needle to avoid significant injury-induced rescue responses. The FGF2-injected rats were compared with either uninjected littermates or those that received intravitreal injection of vehicle alone or FGF2 plus the excess of SR1 as well as rats that were not exposed to constant light. In all cases, the injections were made in the superior hemisphere of the eye. After the indicated time, the animals were killed, and the photoreceptor rescue was quantified as previously described (Goureau *et al.*, 1993) The retinal distribution, binding and processing of FGF2 (^{125}I-FGF2) was examined from 2 h to 2 d after intravitreal injection in the absence or presence of an 80-fold excess of SR1 using light microscopy, cross-linking, and SDS-PAGE analysis.

Quantification of Full-Length FGFR1 and SR1 mRNA Levels

One-twentieth of the RT preparation was used for PCR reaction with Goldstar DNA polymerase (Eurogentec, Seraing, Belgium), 67 mM Tris-HCl (pH 8.8), 16 mM NH_4SO_4, 0.01% Tween 20, 1.5 mM $MgCl_2$, 1 μM primer, 200 μM dNTPs, and 2.5 U/100 μl Goldstar *Taq* polymerase. Each amplification cycle involved denaturation for 30 s at 94°C, annealing for 30 s at 57°C, and primer extension for 35 s at 72°C. Final extension was conducted for 2 min at 72°C. To quantify SR1, we coamplified FGFR1 and SR1 using the following primers: FGF-R1 sense, 5′-ACA ACC CCA GCC ACA ACC C-3′; antisense, 5′-GCA AGC TGG GCT GGG TGT CG-3′; SR1, sense oligomer (ES) was derived from exon 4, 5′-CTG ACA AGG GCA ACT ACA CC-3′; and antisense, IAS. Twenty six cycles of PCR were performed as described above (exponential amplification). The PCR products were subjected to electrophoresis in a 1% agarose gel and transferred to a Hybond N+ membrane (Amersham). Internal oligonucleotides (5′-GGC CAC GAT GCG GTC CAG GTC TTC C-3′ for FGF-R1 and 5′-CGT GGA GTT CAT GTG CAA GG-3′ for SR1) were 5′-end labeled by T4 polynucleotide kinase. The membranes were hybridized in a 10% formamide hybridization buffer for 1 h at 37°C with these ^{32}P-labeled FGF-R1 and SR1 internal primers and then washed in 2× SSC and 0.1% SDS at 55°C and exposed to X-OMAT AR5 x-ray film (Kodak, Rochester, NY).

Quantification of Opsin, FGFR1, and FGF2 mRNA Levels

The following primers were used to coamplify FGFR1, FGF2, and opsin mRNAs in parallel with GAPDH, used as a standard, in 25 (opsin and GAPDH), 28 (FGFR1), or 30 (FGF2) cycles of PCR: opsin: sense, 5′-GCA GCC TAC ATG TTC CTG CT-3′; antisense, 5′-GCA GAC CAC CAC GTA GCG CT-3′; FGF-R1: same as above; FGF2: sense, 5′-GGC TTC TTC CTG CGC ATC CA-3′; antisense: 5′-GCT CTT AGC AGA CAT TGG AAG-3′; GAPDH: sense, 5′-ATG GCA TGG ACT GTG GTC AT-3′; antisense, 5′-ATG CCC CCA TGT TTG TGA TG-3′. PCR products were inserted into the pGEM-T vector (Promega, France) as described above and sequenced. The amount of each PCR product was estimated by electrophoresis in an agarose gel, followed by densitometry and analysis with One D scan software (Biocom, Compaq, Houston, TX).

RESULTS

Nucleotide Sequence of the Rat SR1

Based on the assumption that the mRNA sequence of the full-length rat FGFR1 would be very similar to that of human and mouse, we designed oligonucleotides based on the conserved regions of the FGFR1 sequences of these species. We amplified a 530-bp DNA fragment from Fisher rat retina or purified RPE cell cDNAs by PCR. The sequence of the PCR product was almost identical to that of the FGFR1 rat sequence, with 99% identity between bp 580 and 936 of the rat FGFR1 and no changes in amino acid sequence (our unpublished results). The rat sequence data is available from GenBank under accession number U95164. There were three glycosylation sites at positions 227, 240, and 264 and one tyrosine phosphorylation site at position 307. Nucleotide 936 of the full-length rat FGFR1 (the first codon of exon IIIb or IIIc) is the start of a specific sequence (Figure 1B). This sequence was 72% identical to mouse exon IIIa for the first 230 bp (three point mutations at positions +4, +10, and +15 of the rat sequence and one deletion at position +19 in the coding region of the rat sequence). Rat and human sequences were less similar (24 mismatches and one insertion in a 42-amino-acid coding region) (Figure 1B). The specific rat SR1 sequence codes for 13 additional amino acids followed by a stop codon (Figure 1C). As for the corresponding mouse fragment, but not for the human fragment, this sequence does not encode a complete Ig-like domain. The lack of a hydrophobic stretch of amino acids suggests that this form may be secreted. The amino acid sequence of the rat SR1 was 92% identical to human SR1.

Detection of the SR1 Form in Retina

We raised polyclonal antibodies against the peptide corresponding to the 13-amino-acid sequence from the rat SR1 to investigate the expression of the SR1 in rat

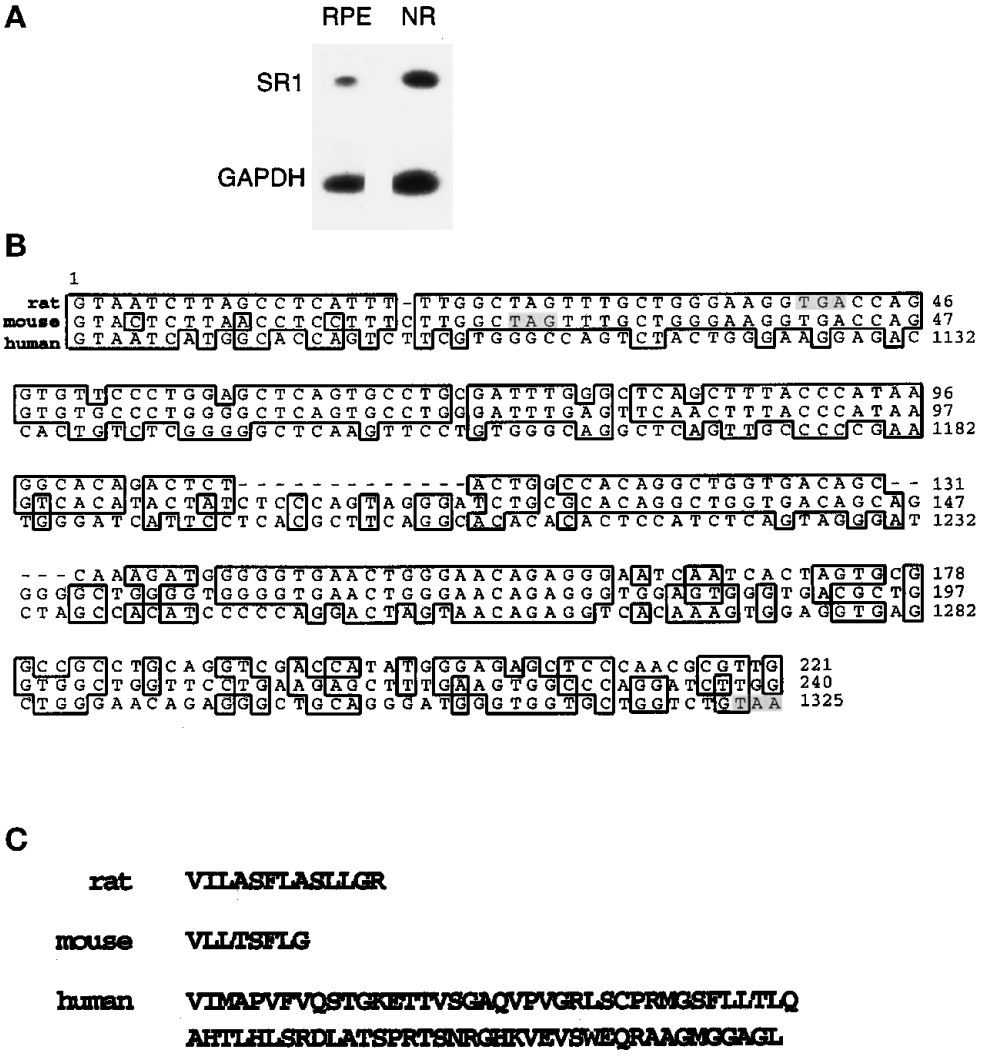

Figure 1. SR1 in rat retina and comparison of rat, mouse, and human sequences. (A) The specific cDNA sequence of SR1 was amplified by PCR from cDNA prepared from neural retina (NR) and purified RPE cell mRNAs as described in MATERIALS AND METHODS. (B) Alignment of rat, mouse, and human coding regions of exon IIIa sequences. This alignment was prepared with Genetics Computer Group (Madison, WI) software using the following sequences, rat (this paper), human SR1 sequence (EMBL M34187, bp 1086–1329) and mouse exon IIIa sequence (EMBL M80363, bp 1–243). Shadowed base pairs represent stop codons of each sequence. (C) Amino acid sequence of rat, mouse, and human encoded by IIIa.

retina. Rat retina extract was immunoprecipitated with anti-full-length FGFR1 antibody (which recognized the peptide corresponding to residues 802–822 of the COOH terminus of the full-length FGFR1 gene product) and anti-SR1 antibody. It was then cross-linked to immobilized ^{125}I-FGF2 on heparin-Sepharose columns, and the complexes were purified and subjected to SDS-PAGE. We detected distinct FGFR1-^{125}I-FGF2 complexes by autoradiography (Figure 2). The antibody directed against the specific 13-amino-acid sequence of SR1 reacted with a major complex at 87 kDa (Figure 2, lane 2). By subtraction of the molecular mass of FGF2 (17 kDa), we deduced that SR1 has a molecular mass of 70 kDa. In contrast, we detected a unique high-molecular-mass band at 170 kDa (Figure 2, lane 3) with the antibody that recognizes the human full-length FGFR1 gene product. This corresponded to the expected size of the full-length membrane-spanning FGFR1–^{125}I-FGF2 complex. As expected, the labeling was completely displaced by the addition of an excess of unlabeled FGF2 and was specifically and completely blocked by incubation of the antibodies with the cognate antigen peptide (our unpublished results).

Distribution of SR1 in Adult Rat Retina

Immunohistochemical studies were performed on adult rat retina sections to analyze the cellular distribution of SR1 (Figure 3). In the absence of Triton X-100, there was moderate anti-SR1 labeling in the optic fiber layer (Figure 3a). Intense anti-SR1 staining was detected in the cell body of the cellular ganglion layer (CGL). There was also anti-SR1 labeling in the inner plexiform layer (IPL) where there are synapses between ganglion cells and the neurons (amacrine, bipolar, and horizontal cells) of the inner nuclear layer (INL). In contrast, the INL and the outer nuclear layer

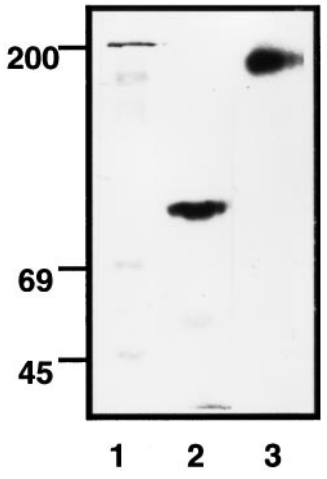

Figure 2. Detection of SR1 and FGFR1 in neural retina. Two hundred micrograms of protein of neural retina extracts of adult rat were bound to ^{125}I-FGF2 heparin-Sepharose. After cross-linking with DSS, proteins were eluted, and immunoprecipitations was performed with antibodies raised against the specific amino sequence of SR1 (lane 2) and against the carboxyl terminus of the full-length FGFR1 (lane 3) as described in MATERIALS AND METHODS. Immunoprecipitated proteins were analyzed by SDS-PAGE on a 10% acrylamide gel and autoradiography. All lanes were run on the same gel, but irrelevant lanes were removed to improve clarity. The gel autoradiograms are representative of three independent experiments.

(ONL) were weakly stained, with faint labeling around neuron nuclei. The inner segments (IS) of the photoreceptors were intensely stained, whereas the outer segments and the interphotoreceptor matrix (IPM) remained unstained. SR1 was also detected in the retinal pigmented epithelium. By using an antibody directed against the specific C-terminal amino acid sequence of human exon IIIa of SR1, we observed a similar pattern of distribution of human SR1 in adult human retina (our unpublished results), indicating that the difference in the C-terminal portion of loop III between rat and human has no consequence on SR1 specificity. In the presence of Triton X-100, which improves antigen accessibility, anti-SR1 staining followed a pattern similar to that observed without Triton X-100, except that the INL was labeled (Figure 3, a, e, i, and k). The three controls for anti-SR1 labeling specificity, incubation of the retina sections with 1) the control preimmune serum (Figure 3b), 2) the anti-SR1 antibody preadsorbed with the cognate antigen peptide (Figure 3c), and 3) omission of the primary antibody (Figure 3d), resulted in no labeling. Using antibodies against specific markers of the various neuronal and nonneuronal cells and by double-staining experiments, we showed that there was no SR1 staining in the vascular endothelial cells (Figure 3, e and h) and in optic nerve fibers (antibody to neurofilament, 68 kDa; Figure 3, e and g). SR1 was not detected in the same areas as glial fibrillary acidic protein, which stained astrocytes of the CGL (Figure 3, i and j). The anti-SR1 antibody intensely stained cell bodies in the CGL where astrocytes and ganglion cells are present, showing that SR1 is present in ganglion cells. In contrast, SR1 staining occurred in the same areas as staining for synaptophysin, which was present in the IPL and OPL (Figure 3, k and l).

Comparison of SR1 Subcellular Distribution with Those of FGFR1, FGF1, and FGF2 in Retina

We detected faint and discrete FGFR1 staining in the inner retina corresponding to the RMG cell end feet with the same anti-full-length FGFR1 antibody as used to detect FGFR1 in retina extracts (Figure 4c). There was also intense staining of the OPL, the photoreceptor IS, and the RPE. Surprisingly, ganglion cells, the cells of the INL, and photoreceptor nuclei were not stained, in contrast to SR1 staining (Figure 4, b and c). Incubation of the anti-full-length FGFR1 antibody with the cognate antigen peptide resulted in no staining (Figure 4f). These data showed that the distribution of SR1 and FGFR1 was clearly different, although both proteins are encoded by the same gene. Immunoreactive FGF1 was detected in the CGL, throughout the INL, and in the RPE cells (Figure 4d). FGF2 immunoreactivity was similar to that of FGF1, but there was also staining of the basement membranes of the retinal capillary endothelial cells of the CGL (Figure 4e, arrow). Incubation of the anti-FGF1 and anti-FGF2 antibodies with the cognate antigen peptide resulted in no staining (our unpublished results).

Changes in Retinal SR1 Synthesis and Distribution During Retinal Degeneration

FGF2 mRNA synthesis and FGF2 protein levels increase in photoreceptors during light-induced retinal degeneration in rat (Gao and Hollyfield, 1995), whereas both FGF2 and full-length FGFR1 mRNA levels increase in rat retina during mechanical injury (Wen *et al*., 1995). This led us to examine whether the increase in FGF2 affected the expression of the various FGF receptor type 1 splice variants. We compared opsin, FGF2, FGFR1, and SR1 mRNA levels over 9 d in light-treated rats, by semiquantitative RT-PCR (Figure 5). After 3 d of exposure to constant light, the level of opsin mRNA decreased to 5% of control values and was accompanied by complete photoreceptor degeneration (Figure 5, A and B). In contrast, after 24 h of light exposure, the FGF2 mRNA level was twice that of the control. The amount of FGF2 mRNA present increased until day 7, when it was 4.7 times that of the control (Figure 5, A and B). The amount of full-length FGFR1 (IIIc) mRNA also increased, up to three to four times that of the control. This level of FGFR1 expression was maintained throughout the 9 d of illumina-

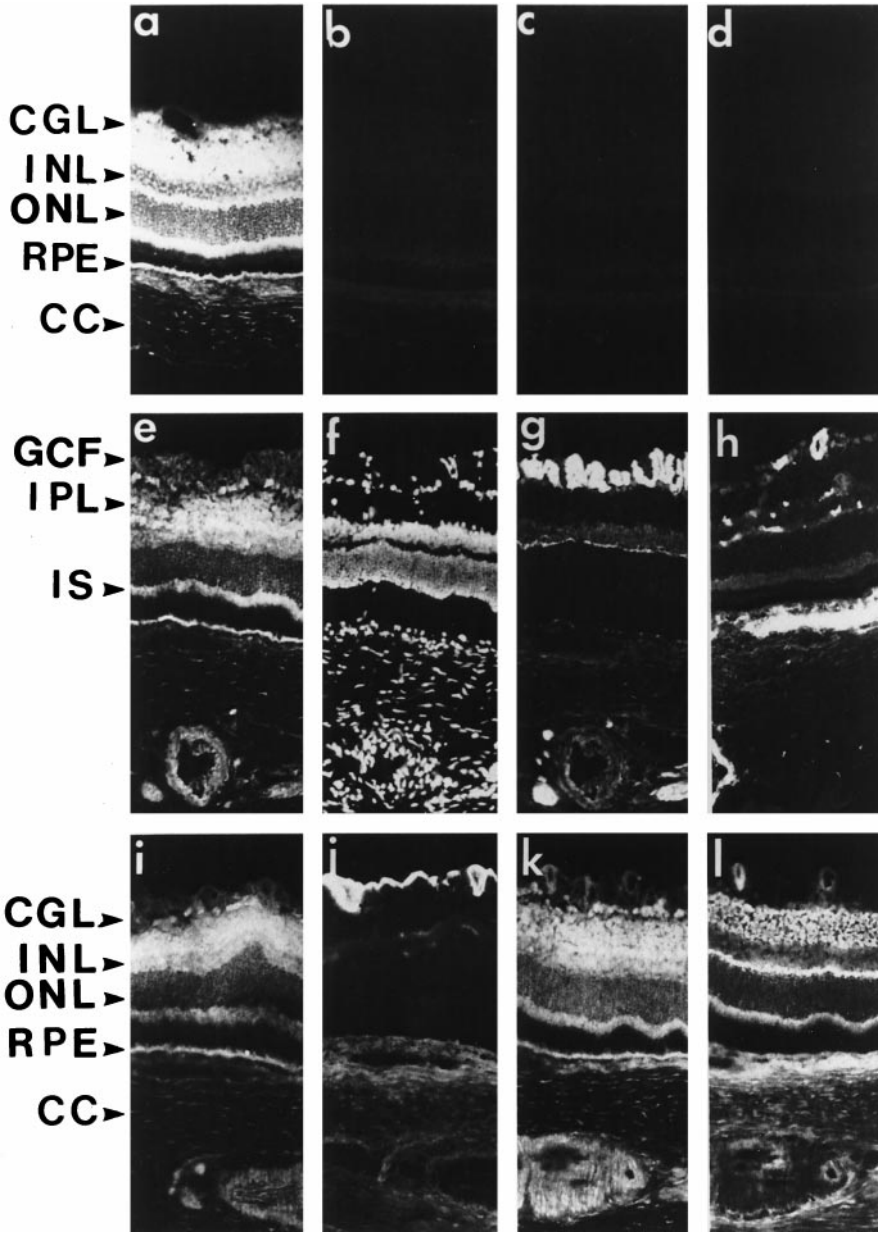

Figure 3. Immunohistochemical distribution of SR1 in retina. Fixed frozen rat retina were permeabilized with Triton X-100 (except in a). The slides were incubated with antibodies using a double-labeling technique (except in a–d and h) as described in MATERIALS AND METHODS. Retina sections (8 μm) were incubated with anti-SR1 antibody (1:250; a, c, e, i, and k), anti-neurofilament 68-kDa antibody (g), anti-factor VIII antibody (h), anti-GFAP antibody (j), and anti-synaptophysin antibody (l), and cell nuclei were stained with DAPI (f). Checks on anti-SR1 labeling specificity: incubation of the retina sections with 1) the control preimmune serum (b), 2) the anti-SR1 antibody preadsorbed with the cognate antigen peptide (c), and 3) primary antibody omitted (d) all gave no labeling. IPL, inner plexiform layer; OPL, outer plexiform layer; ONL, outer nuclear layer; IS, inner segment; RPE, retinal pigmented epithelium; CC, choroid; GCF, ganglion cell fiber. Bar, 55 μm.

tion (Figure 5, A and B). In contrast to the FGFR1 mRNA, the SR1 mRNA level decreased to 30% of control after 24 h of constant light and then increased up to 3.9 times that of the control (Figure 5, C and D). Throughout the illumination period, only the IgIIIc form of the full-length FGFR1 was generated, not the IgIIIb form (our unpublished results).

Retina sections from rats subjected to constant illumination were analyzed by immunochemistry to determine in which cell types the various FGF receptor type 1 splice variants (IgIIIc/IIIa) were located (Figure 6). As previously shown (Ekström *et al.*, 1988), after 24 h of light exposure, an intense anti-GFAP signal was detected in the CGL with less pronounced staining extending into the IPL (Figure 6a). Thereafter, the GFAP signal became stronger within the RMG cell cytoplasm and extended from the end foot region that borders the vitreous cavity to the ONL, indicating sustained activation of RMG cells in response to light injury (Figure 6, b and c). We then assessed production of the full-length FGFR1 (Figure 6, d–f). On day 1, anti-FGFR1 staining was detected in the vitread portion of the RMG cells (Figure 6d). After 5 d, labeling of the full-length FGFR1 was detected in the RMG cell cytoplasm from the end foot to the IPL and was more intense in the photoreceptor nuclei and the RPE (Fig-

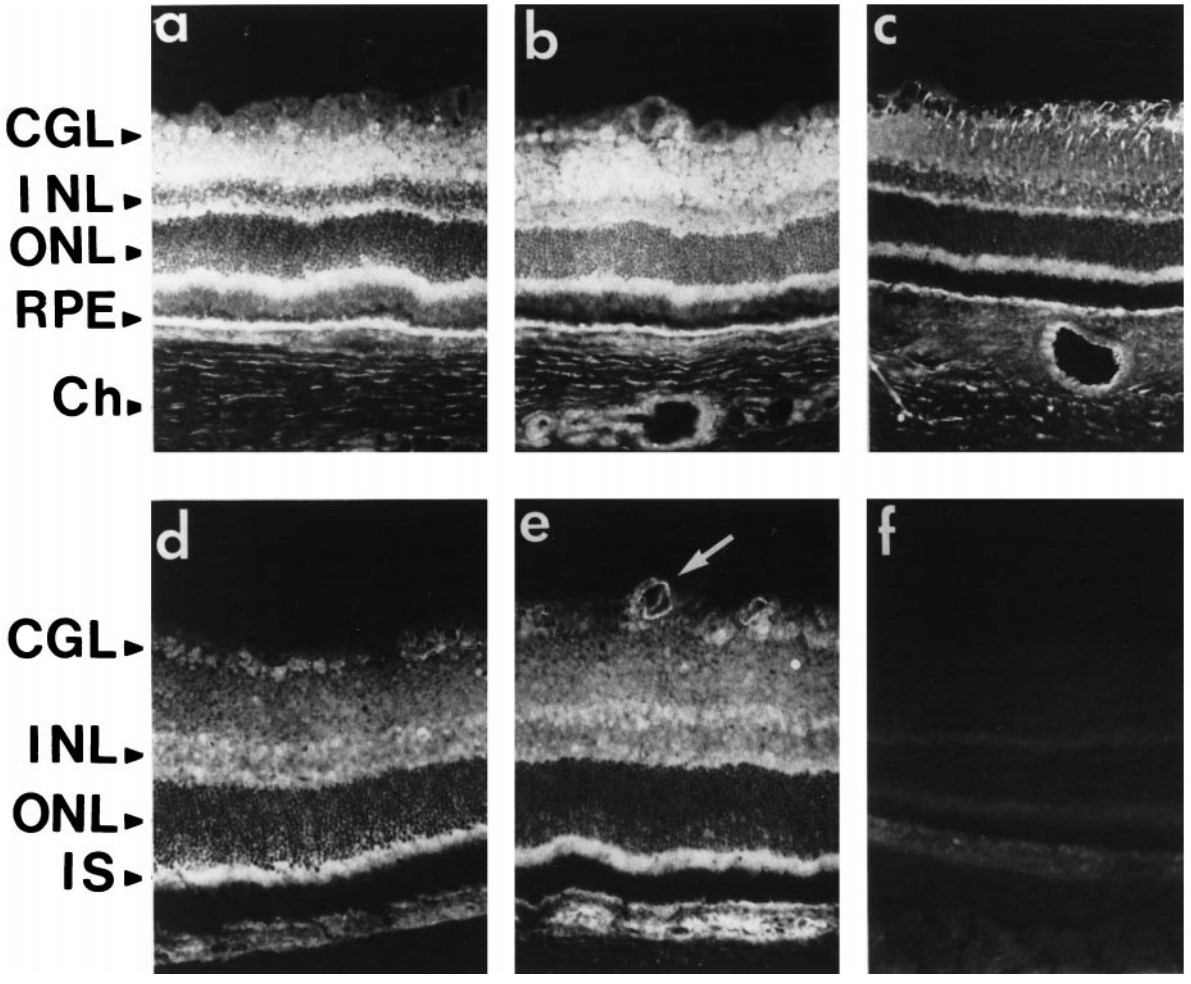

Figure 4. Comparison of SR1 immunoreactivity with FGFR1, FGF1, and FGF2 immunoreactivities in retina. Sections of adult rat retina fixed with 4% paraformaldehyde and permeabilized with Triton X-100 (except in a) were incubated with antibodies against SR1 (1:250; a and b), the carboxyl terminus of FGFR1 (1:200; c), FGF1 (1:100; d), and FGF2 (1:100; e). The white arrow shows FGF2 staining in vascular endothelial cells. GCL, ganglion cell layer; INL, inner nuclear layer; ONL, outer nuclear layer; IS, inner segment; RPE, retinal pigmented epithelium; Ch, choroid. Bar, 70 μm.

ure 6e). On day 9, full-length FGFR1 was detected in RMG cells throughout the IPL and INL. Moreover, there was strong labeling in and around the RPE monolayer (Figure 6f). In contrast, on day 5, intense anti-SR1 labeling was detected in the IPL, in the RPE, and in the apoptotic photoreceptors (Figure 7d). Although there was anti-SR1 staining in the RPE cytoplasm of the control (Figure 7f, white arrow) and of the 1-d–illuminated (Figure 7g, white arrow) rat, anti-SR1 staining increased greatly in RPE after 5 d of illumination (Figure 7h). On day 9, there was less anti-SR1 staining over the neural retina and RPE (Figure 7, e and l). Incubation of the anti-SR1 antibody with the cognate antigen peptide resulted in no staining (Figure 7, a and n).

In summary, during retinal degeneration and photoreceptor apoptosis, we observed a rapid increase in both FGF2 and FGFR1 (IgIIIc) mRNA levels with maximum mRNA synthesis after 7 (for FGF2) and 9 d (for FGFR1) of constant light illumination. In contrast, SR1 (IgIIIa) mRNA levels followed a biphasic pattern of rises and falls. FGFR1 production accompanied gliosis.

Mode of Action of SR1 In Vitro

To gain insight into the function and the mode of action of SR1, we analyzed the functional features of hrSR1 by assessing its effects in vitro on FGF-stimulated RPE cells (the major retinal cell type, which synthesizes both variants of FGFR1). Addition of hSR1 to RPE cells inhibited their proliferative response to FGF1 and FGF2 in a dose-dependent manner (Figure 8A). Maximal inhibition of both FGF1- and FGF2-

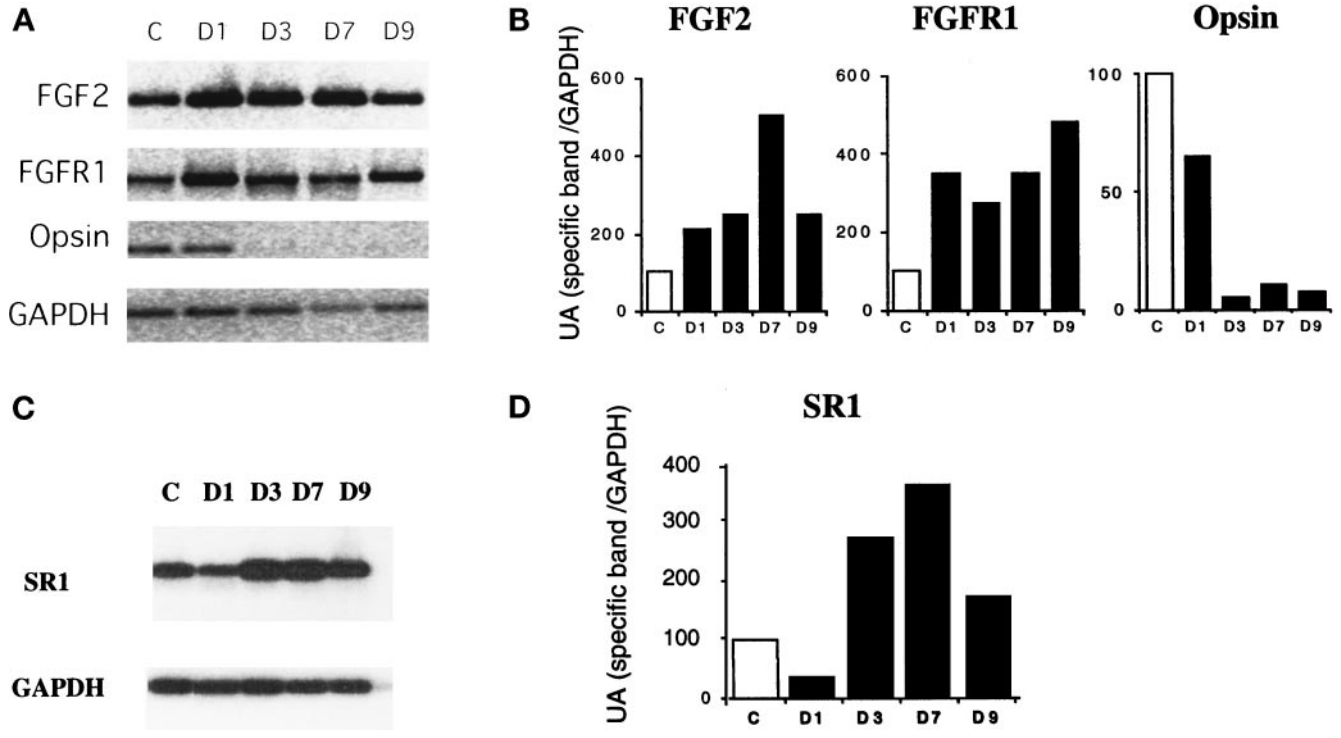

Figure 5. Synthesis of FGF2, FGFR1, and SR1 mRNAs in the retina during retina degeneration. (A) Comparison of FGF2, FGFR1, opsin, and GAPDH mRNA levels over 9 d in light-treated rats by semiquantitative RT-PCR. Retina of nonilluminated rats was the control (c). The time of illumination, in days, is indicated on top of each lane. (B) Quantification of relative PCR products. The amount of PCR products produced was estimated by electrophoresis in an agarose gel followed by densitometry and analysis with One D scan software. (C) Comparison of SR1 and GAPDH mRNA levels over 9 d in light-treated rats by semiquantitative RT-PCR. (D and E) Comparable results were obtained in four independent experiments.

stimulated proliferation was obtained with 1500 ng/ml hrSR1, whereas 50% of maximal inhibition of FGF1- and FGF2-stimulated RPE cells was obtained with 1070 ng/ml (for FGF1) and 520 ng/ml (for FGF2) soluble receptor. Addition of hrSR1 to FGF2-stimulated RPE cells inhibited the long-term FGF2 MAP kinase (ERK2) activation (2 h) of RPE cells (Figure 8A, top panel). The complexity of the interaction of the soluble receptor with RPE cells led us to investigate whether hrSR1 neutralized binding of FGF to FGFR1 in a radioreceptor assay. hrSR1 did not inhibit binding of FGF1 and FGF2 to their low-affinity binding sites (Figure 8B). hrSR1 inhibited binding of both ^{125}I-FGF1 and ^{125}I-FGF2 to the FGFR1 of RPE cells in a dose-dependent manner; 50% inhibition of binding of FGF1 and FGF2 to FGFR1 was obtained with 1210 ng/ml (for FGF1) and 430 ng/ml (for FGF2) hrSR1 (Figure 8C). Direct action of hrSR1 on FGFR1 was demonstrated by cross-linking experiments with ^{125}I-FGF1 and ^{125}I-FGF2 in RPE cells (Figure 8D). In the absence of hrSR1, a single ^{125}I-FGF2–FGFR1 complex (Figure 8D, lane 1) and a single ^{125}I-FGF1–FGFR1 complex (Figure 8D, lane 2) were observed (black arrow). The specificity of the formation of these complexes was demonstrated by the addition of excess unlabeled FGF1 and FGF2 (Figure 8D, lanes 3 and 4). Addition of 700 ng/ml hSR1 to ^{125}I-FGF2 or ^{125}I-FGF1 abolished the formation of the FGFR1–^{125}I-FGF complex (Figure 8D, lanes 5 and 7). We did not detect any higher-molecular-mass complex in the presence of hrSR1, suggesting that the iodinated FGF–SR1–FGFR1 complex did not form. The specificity of the inhibitory effect of hrSR1 on the binding of FGFs to FGFR1 was demonstrated by incubation of hrSR1 with an excess of unlabeled FGF2 and FGF1 (Figure 8D, lanes 6 and 8).

In Vivo Effects and Mode of Action of SR1

Intravitreal injection of FGF2 rescues photoreceptors from the damaging effects of constant light in the rat (Faktorovich *et al.* 1992). To determine whether SR1 could modulate the in vivo FGF2 protective role of photoreceptor during light-induced retina degeneration, we compared the effects of intravitreal injection of FGF2 with intravitreal injection of FGF2 in the presence of an 80-fold excess of SR1 (Figure 9).

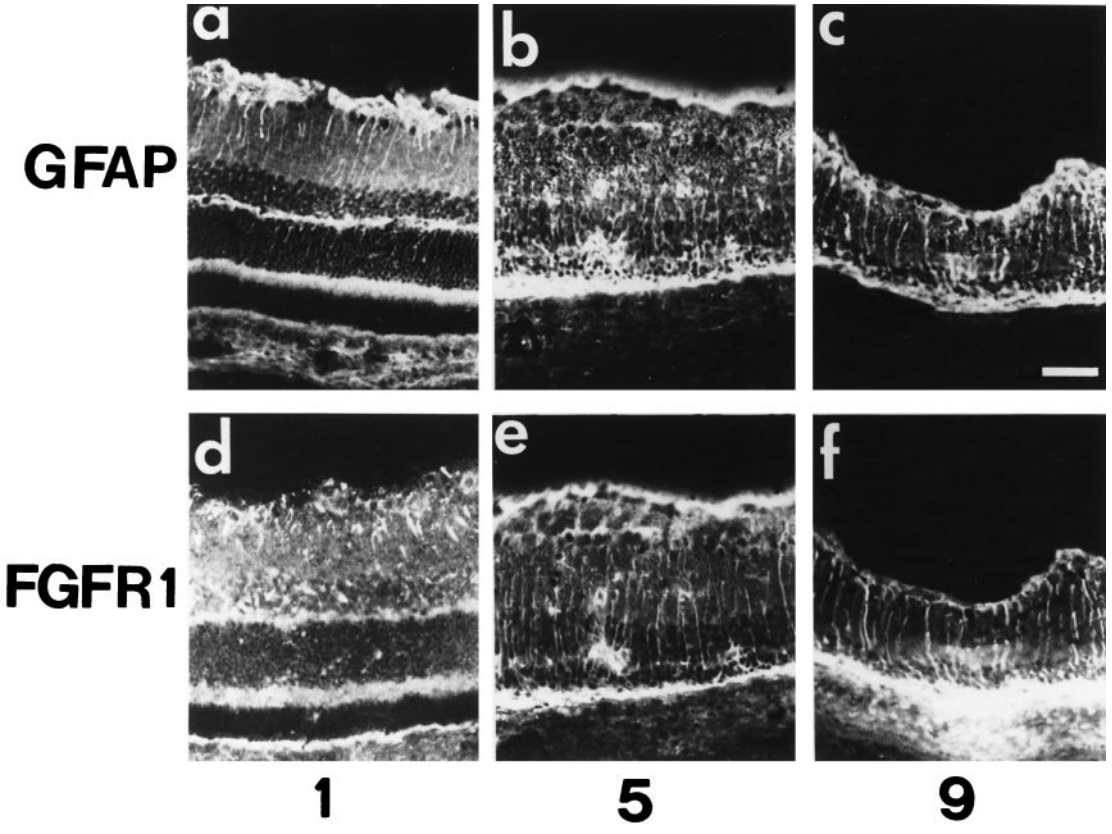

Figure 6. Immunolocalization of glial fibrillary acidic protein and the full-length FGFR1 in light-induced retina degeneration. Immunohistochemical study of retina of adult rats exposed to constant light for 1 d (1), 5 d (5), and 9 d (9), probed with anti-GFAP antibodies (a–c) and with anti-carboxyl terminal FGFR1 antibodies (d–f), was performed as described in MATERIALS AND METHODS. Note the increase in GFAP immunoreactivity in the inner nuclear and plexiform layers after 5 d of constant illumination in b and c. This staining colocalized with FGF-R1 immunoreactivity (e and f). Bar, 70 μm.

After 3 d in constant light, uninjected rats showed a loss of most photoreceptors in the superior region of the retina (Figure 9b). Light damage was more pronounced after 5 d of constant illumination (Figure 9c). The ONL was reduced from the normal 9–11 rows of photoreceptor nuclei to 2–5 rows, the IS were very small, and no outer segments of normal length were observed. After 7 d, the ONL consisted of one or two rows of nuclei, but there was no obvious damage to the RPE (Figure 9d). The INL and the IPL were also intact. In contrast, eyes of rats exposed to constant light for 5 d beginning 2 d after intravitreal FGF2 injection were not degenerated (Figure 9g). After 7 d of constant light, retinas were less degenerated than in uninjected eyes exposed to the same period of constant light (Figure 9h). In these retinas, the ONL was 60–70% of the normal thickness and twice as thick as in the contralateral light-damaged control uninjected eye or in the eye injected with the vehicle. Those rats that were injected with vehicle and subjected to constant light showed retinas that were quantitatively indistinguishable from those of uninjected light-damaged rats (our unpublished results). After only 3 d of constant illumination, coinjection of an excess of SR1 with FGF2 appeared to inhibit the protective activity of FGF2 on photoreceptor degeneration (Figure 9j). The ONL was reduced to four or five rows of photoreceptor nuclei, and the inner and outer segments were more damaged than in the eyes injected with the vehicle alone or with heat-denatured FGF2. After 5 d of constant illumination, retinas showed no rescue, ONL measurements were greatly less (two or three rows of photoreceptor nuclei) than after FGF2 injection ,and photoreceptor integrity appeared identical to the control of uninjected illuminated eye (Figure 9k). Surprisingly, on day 7, the ONL disappeared completely, and the INL was greatly reduced (Figure 9l). Coinjection of FGF2 with an excess of heat-denatured SR1 (biologically inactive in in vitro mitogenic and radioreceptor assays) did not alter the protective activity of FGF2 (our unpublished results).

Because it has been speculated that increased gene expression of FGF2 in light-induced retinal degeneration may function as a protective response of the ret-

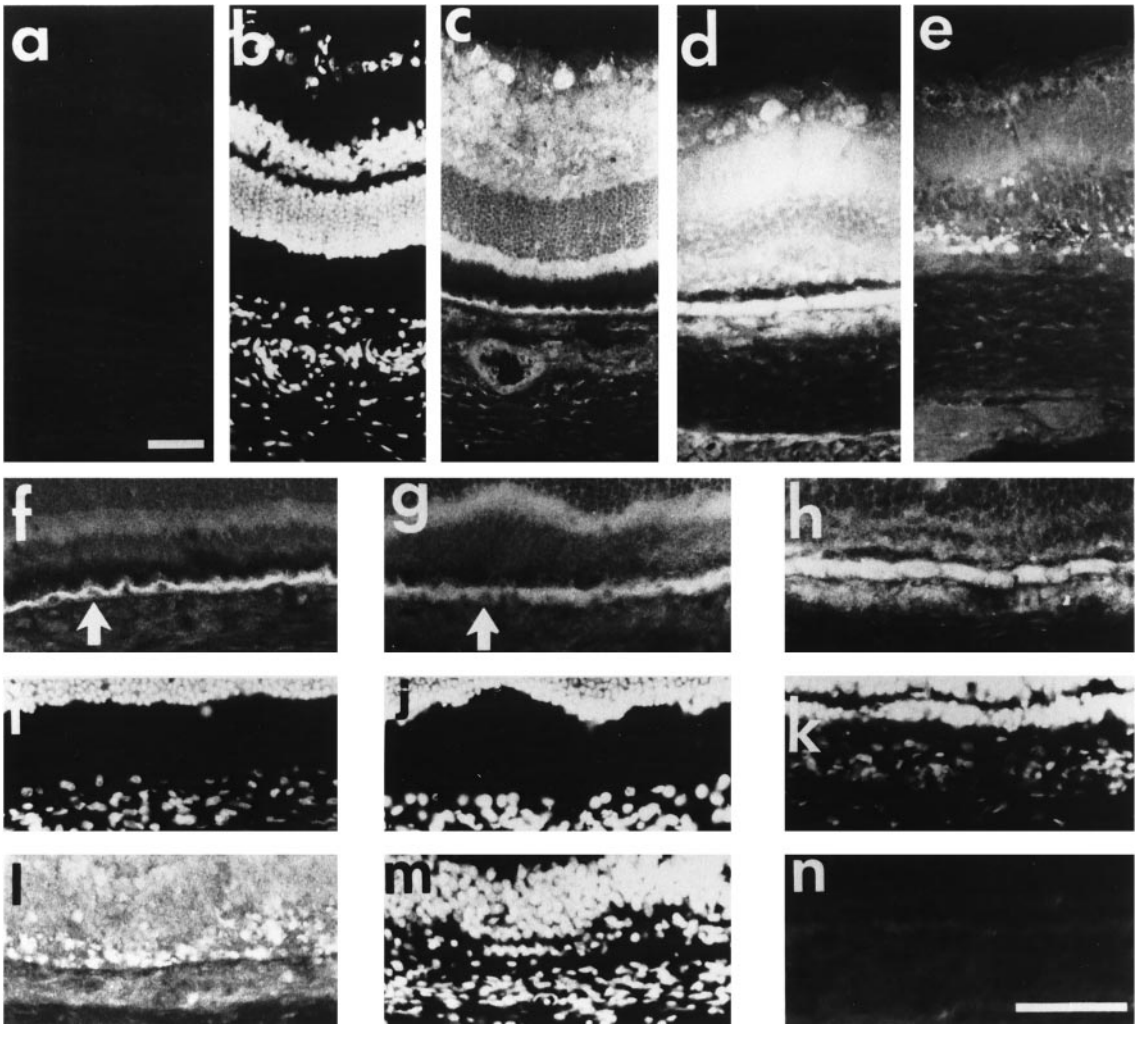

Figure 7. Immunolocalization of SR1 in light-induced retina degeneration. Immunohistochemical study of retina of nonilluminated control adult rats (a–c, f, and i) and of rats illuminated for 1 d (g and j), 5 d (d, hm and k) and 9 d (e, l, and m), probed with anti-SR1 antibody. Cell nuclei were stained with DAPI (b, i–k, and m). Note the absence of specific staining with the anti-SR1 antibody preadsorbed with the cognate antigen peptide (a and n). (f–n) Nuclear immunolocalization of SR1 in RPE on day 5 of constant illumination; note the absence of SR1 immunostaining in RPE cell nuclei in the control (f and i) and in 1-d–illuminated (g and j) rat (white arrow), whereas in 5-d–illuminated rat (h and k) SR1 was detected in the cytoplasm and in the nucleus of RPE cells. Bars, 55 μm.

ina to photoreceptor stress (Gao and Hollyfield, 1996), we analyzed the effects of a single injection of SR1 alone. When rats were exposed to constant light for 1 d beginning 2 d after intravitreal SR1 injection, photoreceptor degeneration was more extensive than in uninjected eyes and in eyes coinjected with SR1 and FGF2 exposed to the same period of constant light (Figure 9m). On day 3 of illumination, the ONL was thinner than in corresponding regions of retinas in uninjected eyes (Figure 9n). In addition, we observed a marked reduction in the INL. After 5 d of constant light, retinas of SR1-injected eyes were more degenerated than those in uninjected eyes and in eyes coinjected with FGF2 and SR1 after 7 d of light exposure (Figure 9o). The ONL was reduced to one row of photoreceptor nuclei, and the INL was at least 50% the normal thickness of the contralateral light-damaged control eye that received heat-denatured SR1 injection. After 7 d of constant light, there was a dramatic retina degeneration that was never observed in uninjected eyes (Figure 9p). Both the ONL and the INL disappeared, and only the ganglion cell layer was present.

Because we showed that SR1 abolishes the in vitro FGF2 biological activity by inhibiting FGF2 binding to FGFR1, we postulate that in vivo, SR1 coinjected with FGF2 could inhibit the neurotrophic activity of FGF2 by inhibiting the binding of exogenous FGF2 to endogenous retinal FGFRs. To analyze the mode of ac-

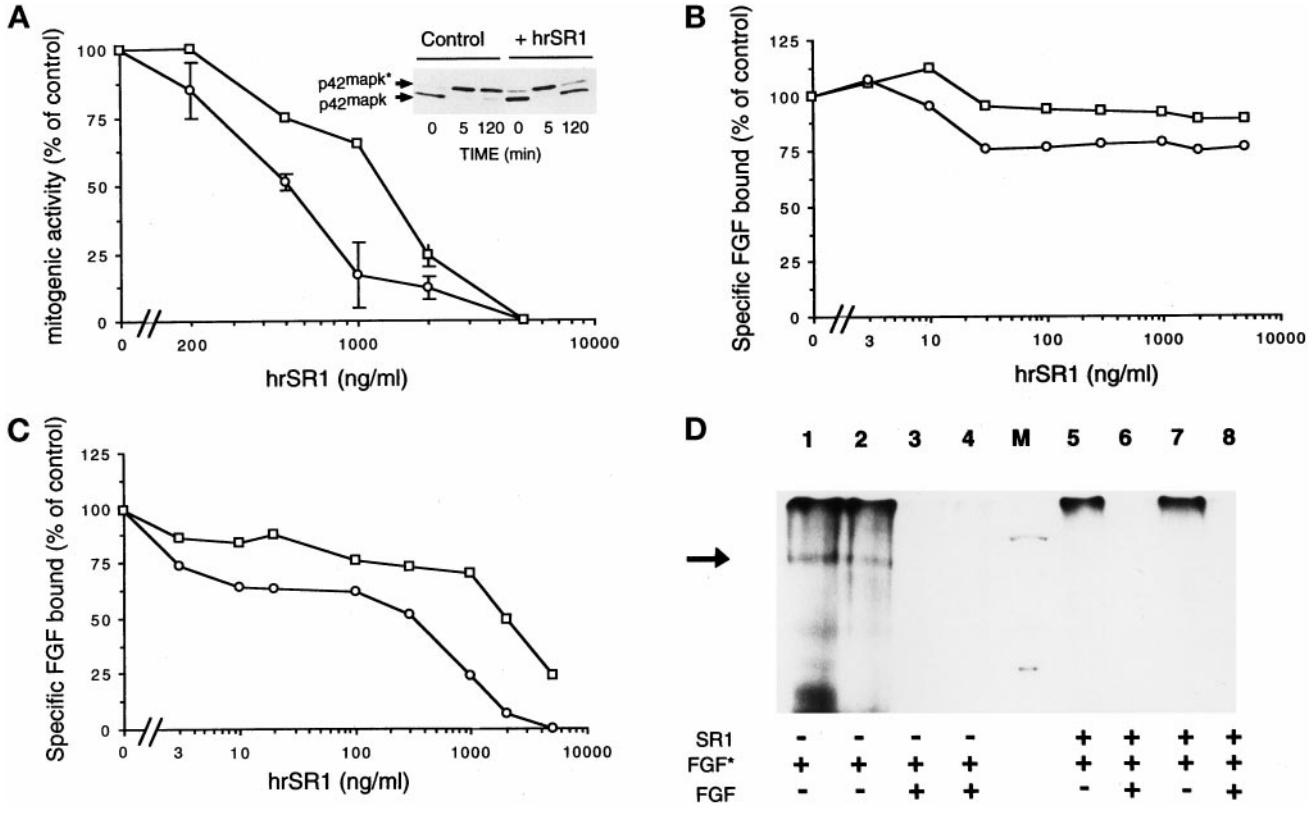

Figure 8. In vitro effects of hrSR1 on FGF1- and FGF2-induced mitogenesis and ERK2 activation and on FGF1 and FGF2 binding in RPE cells. (A) RPE cells were incubated with varying concentration of human recombinant SR1 (hrSR1) in the presence of FGF1 (□) and of FGF2 (○) at 10 ng/ml. Mitogenic activity was measured by the incorporation of tritiated thymidine. The percentage of inhibition of activity is plotted as a function of the hrSR1 concentration. (A, top panel) ERK2 phosphorylation was detected by its characteristic retardation of electrophoretic mobility. The phosphorylated (ERK2*) and unphosphorylated (ERK2) forms of MAP kinase are indicated. (B and C) RPE cells were incubated with ^{125}I-FGF1 (□) and ^{125}I-FGF2 (○) at 5 ng/ml in the presence of various concentrations of hrSR1. The amount of ^{125}I-FGF bound to high-affinity receptors (C) was measured in Triton X-100 cell extracts after cells were washed with 2 M NaCl. The radioactivity in the 2 M NaCl washes was ^{125}I-FGF bound to the FGF low-affinity binding sites (B). Nonspecific binding of ^{125}I-FGF to RPE cells was determined in the presence of an excess of unlabeled FGF (200-fold). No error bar is given for points, because the errors were smaller than the symbols. (D) Cross-linking of ^{125}I-FGF1 (lanes 2, 4, 7, and 8) and ^{125}I-FGF2 (lanes 1, 3, 5, and 6) to RPE cells. Cells were incubated with 5 ng/ml iodinated FGF (FGF*) in the presence of 700 ng/ml hrSR1 (lanes 5–8). Checks of the specificity of iodinated FGF binding in the presence of hrSR1: cell incubation with an excess of unlabeled FGF1 (lanes 4 and 8) and unlabeled FGF2 (lanes 3 and 6). Cross- linking was performed as described in MATERIALS AND METHODS. A specific band was detected at 170 kDa (black arrow). M, molecular mass markers (200, 92, and 69 kDa). In all assays, comparable results were obtained in three independent experiments.

tion of SR1 in vivo, we studied the binding, internalization and the retinal distribution of intravitreal injected ^{125}I-FGF2 in the absence and in the presence of an 80-fold excess of SR1. Retinas obtained from eyes that had been injected with ^{125}I-FGF2 were incubated with the homobifunctional cross-linker BS3. As shown in Figure 10A, examination of an autoradiogram of solubilized cellular extract showed the presence of an FGF2–FGFR complex with an apparent molecular mass of 160 kDa. The labeling was completely displaced by the addition of the excess SR1. In eyes injected with ^{125}I-FGF2 plus an excess of unlabeled FGF2, the 160-kDa band was also displaced (our unpublished results). Retinas from ^{125}I-FGF2–injected eyes with or without an excess of SR1 were dissected at 2, 6, 24, and 48 h after injection, and the internalization and processing of FGF2 were analyzed after SDS-PAGE and autoradiography. Two hours after injection of FGF2, the 17.5-kDa native form of FGF2 was the only peptide observed (Figure 10B). At 6 h, a minor 16-kDa fragment appeared, which continued to accumulate, indicating a degradation of FGF2 within the retina. At 24 h after injection, in addition to the 16-kDa peptide, 9- and 5-kDa fragments appeared, which accumulated until 48 h. In contrast, addition of an excess of SR1 to ^{125}I-FGF2 inhibited FGF2 internalization.

By light microscopy, we analyzed the distribution of ^{125}I-FGF2 on retina sections of rats injected with ^{125}I-FGF2 in the absence and presence of SR1. Intra-

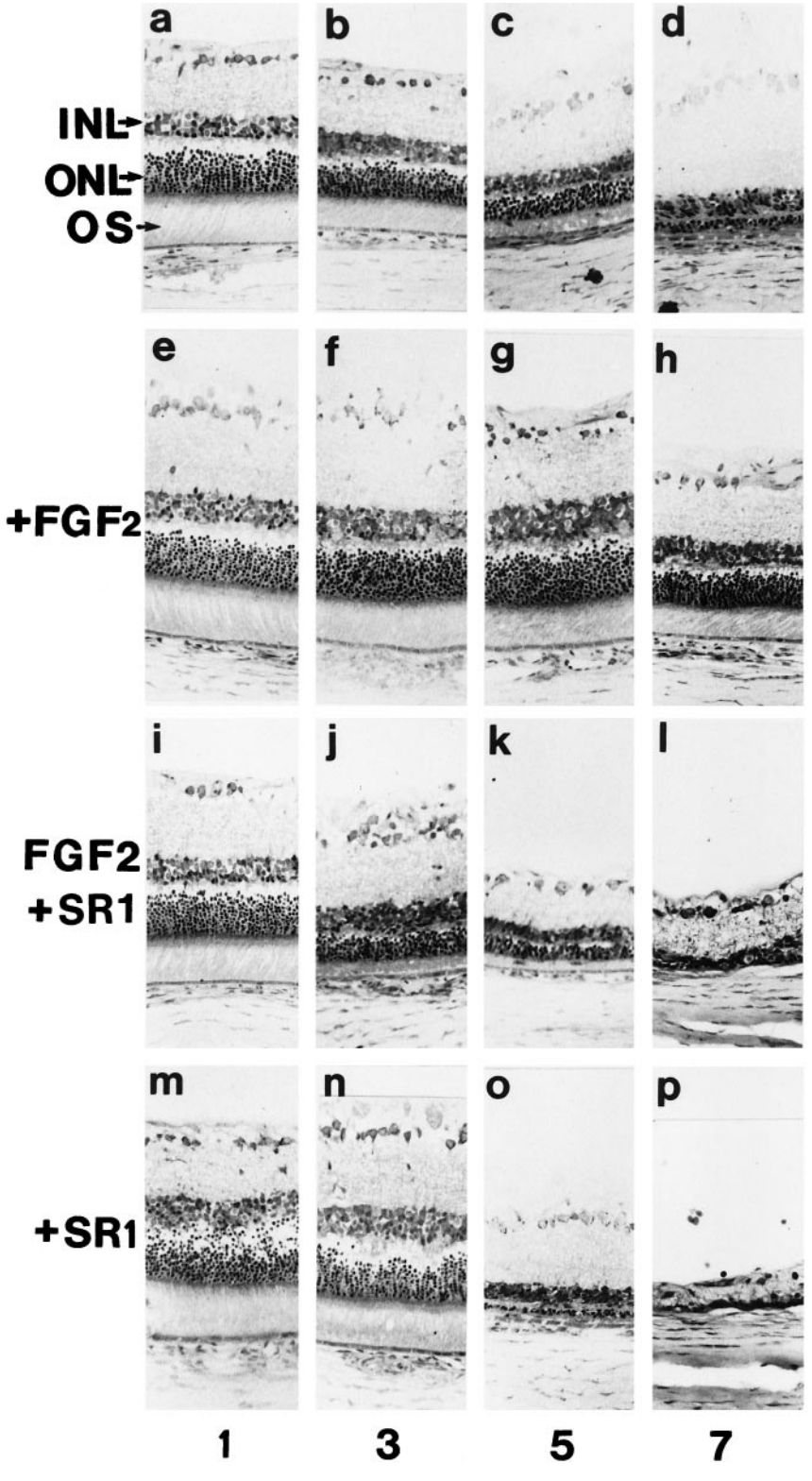

Figure 9. In vivo effects of SR1 during light-induced retinal degeneration and on the FGF2 protection from light damage: light micrographs of retinas from F 344 albino rats taken from the posterior superior region of the eye. (a–d) Retinas from uninjected rats exposed to constant light. (e–h) Retinas from rats injected intravitreally with FGF2 (250 ng) 2 d before constant light. (i–l) Retinas from rats injected intravitreally with FGF2 (250 ng) plus an excess of 80-fold SR1 2 d before constant light. (m–p) Retinas from rats injected with SR1 (20 μg) 2 d before constant light. Numbers refer to the time (in days) of constant illumination INL, inner nuclear layer; ONL, outer nuclear layer; OS, outer segment. Bar, 70 μm. In all assays, comparable results were obtained in three independent experiments.

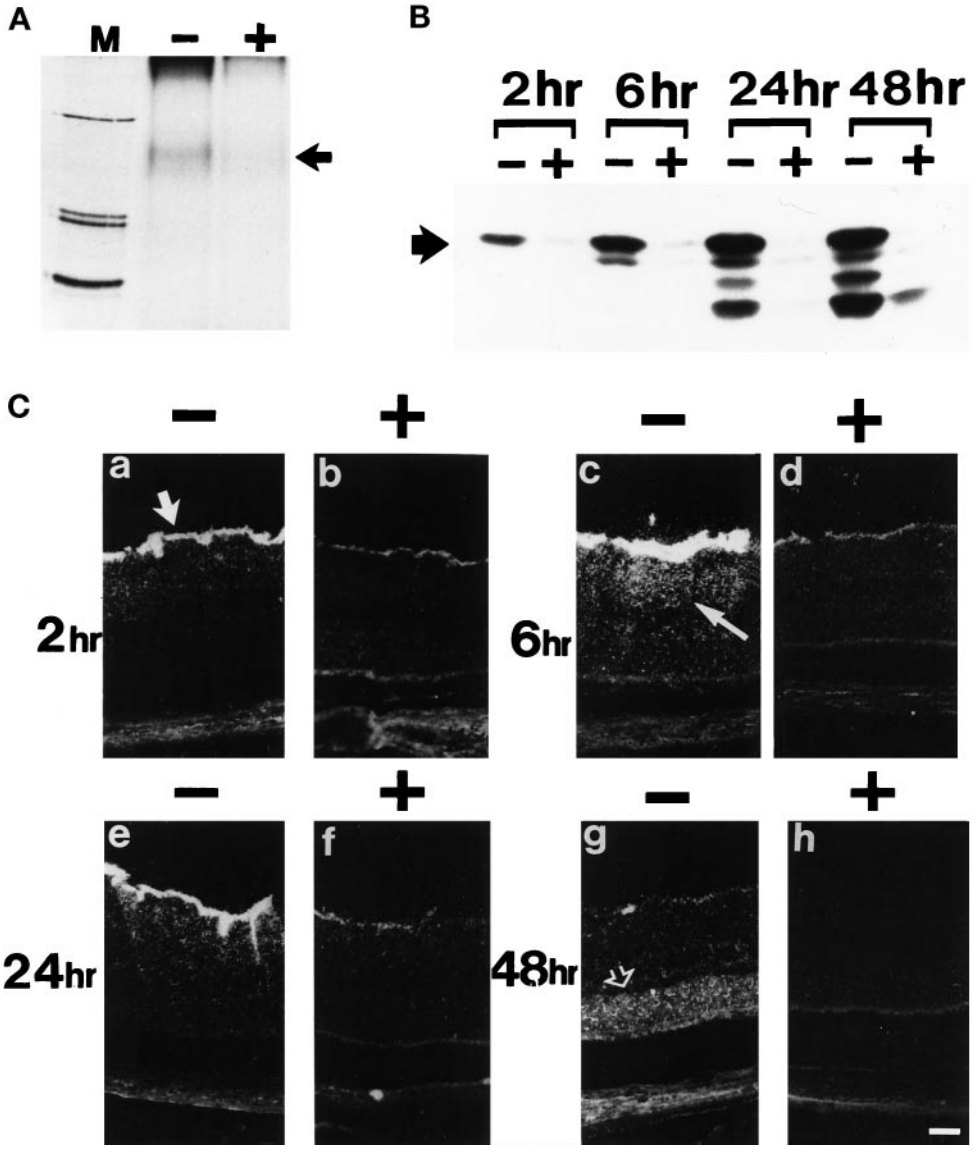

Figure 10. In vivo effects of SR1 on exogenous FGF2 binding and internalization in normal retina. (A) Cross-link of retinal extract with injected ^{125}I-FGF2 in the absence (+) and presence (−) of an excess of SR1. A specific band was detected at 160 kDa (black arrow). M, molecular mass markers (200, 92, and 69 kDa). (B) Internalization and processing at 2, 6, 24, and 48 h after injection of ^{125}I-FGF2 injected in the absence (−) and presence (+) of an excess of hrSR1. The black arrow shows intact ^{125}I-FGF2. (C) Dark-field micrographs from F344 albino rats injected intraviteally with ^{125}I-FGF2 in the absence (−) and presence (+) of an excess of hrSR1 and observed at 2, 6, 24, and 48 h after injection. At 2 h, labeling appeared in the ganglion cell layer (large white arrow) and then diffused in the inner nuclear (thin white arrow) and plexiform layers at 6 h. At 48 h, labeling was mainly present in the ONL (open white arrow). Comparable results were obtained in three independent experiments.

vitreal injection of ^{125}I FGF2 resulted in the radiolabeling of the retina. Two hours after injection of ^{125}I-FGF2, labeling appeared to be primarily in the vitreous and on the inner limiting membrane. Radiolabeling was mainly associated with the nerve fibers of the ganglion cells, the astrocytes, the end feet of the RMG cells, and the basement membranes surrounding the blood vessels (Figure 10C). In addition, a diffuse labeling was present in the INL and the IPL. At 6 h after injection, the labeling associated with the inner limiting membrane and in the INL was stronger, whereas a punctuate labeling appeared for the first time in the ONL and in the IS of the photoreceptors. After 24 h, the radiolabeling persisted along the inner limiting membrane and in the INL and was detected in the RMG cell processes. At 48 h after injection, the labeling along the inner surface of the retina disappeared, whereas it decreased in the INL. In contrast, widespread labeling increased in the ONL. Coinjection of an 80-fold excess of SR1 with ^{125}I-FGF2 showed that SR1 blocked almost completely the labeling in the retina. At 2, 6, 24, and 48 h after injection, only traces of radiolabeling could be detected at the inner surface of the retina, whereas labeling was still detectable in the vitreous. Interestingly, coinjection of SR1 with FGF2 did not inhibited FGF2 binding to the basal membrane of the lens, implying that SR1 did not modify FGF2 diffusion in the vitreous and FGF2 binding to its low-affinity sites. In ^{125}I-FGF2 coinjected with an excess of 200-fold unlabeled FGF2

eyes, the labeling pattern in the retina was similar to the pattern obtained in ^{125}I-FGF2 coinjected with an excess of 80-fold of SR1 eyes (our unpublished results).

DISCUSSION

Cell Specificity of the Various FGFR1 Forms in the Retina

Soluble binding proteins have been reported for various growth factors and cytokines. These proteins are often derived by alternative splicing of exons encoding full-length membrane-spanning receptors, whereas other binding proteins are generated by mechanisms involving proteolysis.

In this report, we demonstrated that mature rat neural retina synthesizes two forms of fibroblast growth factor receptor type 1 in vivo. The prototype form is the full-length FGFR1 (150 kDa), which was detected by an antibody directed against the COOH-terminal sequence of the full-length FGF-R1 gene product. Using RT-PCR, we purified and sequenced a new FGFR1 variant generated by alternative transcription of the FGFR1 gene in rat. The amino acid sequence of SR1 is identical to that of the full-length FGFR1, except that the coding region terminated at the carboxyl-end of the third Ig domain. Thus, SR1 is a secreted protein containing a specific 13-amino-acid sequence, which is absent in the full-length FGFR1 form. This sequence of the protein product differs considerably in rat, mouse, and human (Johnson *et al.*, 1991; Werner *et al.*, 1992). The reason for this difference is unknown. But the difference in the sequence of the third Ig domain does not modify the capacity of rat SR1 to bind to FGF2. SR1 protein was detected after immunoprecipitation with the antibody raised against the specific 13-amino-acid sequence preceding the coding region of the polyadenylation site by two techniques: by binding to FGF2 immobilized on heparin-Sepharose columns and by ligand blotting with FGF2. Our data on rat SR1 are confirmed by previous studies on mouse SR1, showing that despite the lack of an important portion of the third Ig domain, mouse SR1 was able to bind to FGF1 and FGF2 (Werner *et al.*, 1992). Numerous controls were made of the specificity of the anti-SR1 antibody to show that this low-molecular-mass FGFR1 variant (70 kDa) was effectively a form of soluble truncated FGFR1: 1) immunoprecipitation with antibody preadsorbed with the cognate antigen peptide, 2) cross-linking in the presence of unlabeled FGFs, and 3) ligand blotting with specifically blocked antibody after preadsorption with the cognate antigen-peptide.

FGF-BPs have been detected in human retina (Hanneken *et al.*, 1995). These 85- and 55-kDa proteins were detected by immunoblotting using antibodies raised against the extracellular domain of the full-length FGFR1, and such results are consistent with our detection of SR1 in rat retina. The mechanism by which the various low-molecular-mass forms of FGFR1 are generated in human retina is not known, but proteolysis may have an important role. Recently it was shown that gelatinase A, a matrix metalloproteinase, hydrolyzes a specific amino acid sequence upstream from the transmembrane domain of the FGFR1 ectodomain (Levi *et al.*, 1996). Based on these findings, FGF-BPs in human retina may be generated by specific proteolytic cleavage of the full-length FGFR1. This is supported by data showing that human forms FGF-BPs are located in the extracellular matrix of retinal capillary endothelial cells (Hanneken *et al.*, 1995).

Using an antibody that recognized the carboxyl terminus of the human full-length FGFR1, the strongest staining was detected in the inner part of the retina, corresponding to the vitreal portion of the RMG cells. Intense staining was also detected in the basement membranes of blood vessels and of retina capillary endothelial cells. Hanneken *et al.* (1995), using a different antibody to the carboxyl terminus of human FGFR1, also detected immunoreactive FGFR1 in the inner retina and in the basement membranes of retinal capillary endothelial cells. The pattern of SR1 production was different from that of the full-length FGFR1, suggesting a specific role for SR1 in the retina. The strong immunoreactivity of SR1 in the IPL suggests that this protein may be involved in neuronal transmission. This is consistent with the colocalization of SR1 with synaptophysin immunoreactivity. Cell permeabilization revealed SR1 immunoreactivity in the INL, suggesting a difference in the subcellular distribution of SR1 between the second-order neurons and the neurons of the rest of the retina. Unlike human FGF-BPs, there was no SR1 in the basement membranes of the retinal vasculature in rats, suggesting a difference in the generation, role, or mode of action of these two forms of truncated FGFR1. In addition, no SR1 staining was detected in the rat IPM, in contrast with previous studies showing the presence of FGF-BPs in biological fluids (Hanneken and Baird, 1995). These data suggest there are differences between SR1 and FGF-BPs. It will be of interest to study the presence of FGF-BPs in IPM. Furthermore, FGF1 and SR1 immunoreactivities colocalized to CGL, INL, IS, and RPE, whereas FGF2 immunoreactivity colocalized with FGF-BPs in the basement membrane of the retinal vasculature (Hanneken *et al.*, 1995). This suggests that SR1 and FGF-BPs may have also different ligand specificity. This is consistent with the greater inhibitory effect of SR1 on FGF2-induced proliferation and FGF2 binding in RPE cells and is consistent with previous work showing that the human soluble receptor preferentially binds FGF2 over FGF1 (Duan *et al.*, 1992).

Specific Regulation of the Various FGFR1 Forms during Photoreceptor Apoptosis

The rationale for exploring the effects of exposure to constant light on the two FGFR1 transcripts arose from the observations that 1) light induces FGF1 release from photoreceptors (Mascarelli *et al.*, 1989); 2) FGF2 mRNA levels increase after a variety of rat and mouse photoreceptor insults in both inherited and light-induced retina degeneration (Gao and Hollyfield, 1995); 3) In rd mice, after photoreceptor degeneration, FGF2 gene expression increases in photoreceptors and in INL (Gao and Hollyfield, 1996); 4) a single-point focal mechanical injury in rat retina leads to a substantial and persistent increase in FGF2 mRNA synthesis and a transient increase in FGFR1 mRNA (Wen *et al.*, 1995); and 5) overproduction of FGF2 in vitro results in higher FGFR1 mRNA levels but not in higher levels of FGFR2 and FGFR3 mRNAs (Estival *et al.*, 1996). In addition, experimental retinal degeneration induced by light provides a relatively simple and efficient system for the in vivo assessment of the photoreceptor survival-promoting or -inhibiting activity of various agents.

Shortly after exposure to constant light, FGF2 was overproduced (present data). Immunohistochemistry showed that it was located in the vicinity of photoreceptor nuclei, in IS of photoreceptors (Gao and Hollyfield, 1996). The amount of the full-length FGFR1 mRNA (IIIc) also increased and remained high for the entire study period, suggesting that FGF2 may activate FGFR1-bearing cells. In addition, the full-length FGFR1 and GFAP colocalized to RMG cells. This indicates that FGFR1 is overproduced during Muller cell activation after retinal light damage. This important regulatory response of a nonneuronal cell to photoreceptor degeneration may be caused by the increase in FGF2 production, because FGF2 regulates the proliferation and GFAP synthesis of RMG cells (Lewis *et al.*, 1992). During retina degeneration, both SR1 mRNA synthesis and its subcellular localization change, but in a different way than in FGFR1. The biphasic rise and fall of SR1 mRNA synthesis occurred at a time when FGFR1 mRNA was being continuously synthesized, showing the independence of polyadenylation site use and the alternative splicing of the IIIc transcript. This result strongly suggests a specific role for SR1, distinct from that of the full-length FGFR1.

Does SR1 Have Specific Roles and Modes of Action?

Generally, truncated forms of cytokine, growth factor, and neurotrophin receptors inhibit the biological effects of their ligands. In the nervous system, soluble receptors can have an important role in clearing ligands, preventing overstimulation of cell-bound receptors (Friesen *et al.*, 1993). The precise functions in vivo of any of the previously described FGF-BPs and of SR1 are unknown. Several hypotheses can be put forward to explain our results and those of previous studies on truncated soluble and truncated transmembrane FGF receptors.

Because SR1 binds FGF1 and FGF2, we suggested that SR1 may function as an antagonist of FGFs by sequestering excess FGFs produced after cell damage in normal or pathological situations such a neuronal injury. In this case, SR1 would be involved in competition for ligand binding with transmembrane receptors. Using two complementary techniques (radioreceptor assay and cross-linking) our in vitro study clearly demonstrated that SR1 inhibits FGF mitogenic activity by preventing FGF binding to FGFR1, whereas the in vivo experiments showed that SR1 blocks FGF2 neurotrophic activity in the retina by inhibiting FGF2 binding to FGF tyrosine kinase receptors and its subsequent internalization. The absence of any high-molecular-mass complexes corresponding to FGF–SR1–FGFR1 suggests that SR1 may not exist as a dominant negative partner for the full-length FGFR1, in contrast to the truncated transmembrane FGF receptor. In vitro studies have shown that recombinant soluble FGFR forms compete with their cellular transmembrane counterparts for ligand binding in a dose-dependent manner (Duan *et al.*, 1992; Bergonzoni *et al.*, 1993; Caccia *et al.*, 1993), but only at high concentrations (up to 500–1000 ng/ml). During retinal degeneration, we observed SR1 overproduction when FGF2 was also overproduced. This is consistent with the notion of overproduction of SR1 to prevent cell stimulation caused by overproduced FGFs during retinal degeneration. Our results on the increased gene expression and protein production of SR1 during light-induced retinal degeneration also explain why only massive intravitreal injection of FGF2 could rescue photoreceptors, whereas FGF2-increased gene expression in retina failed to show any rescue effects. This hypothesis is confirmed by the strong and rapid degenerative effect of SR1 injected 2 d before constant illumination, demonstrating that SR1 also inhibited endogenous FGF2.

Cell transfection with cDNA encoding truncated transmembrane forms of FGFR blocks the FGF response by the formation of nonfunctional FGFR heterodimers and by the inhibition of the transphosphorylation of FGFR (Ueno *et al.*, 1992; Li *et al.*, 1994). Thus, the mechanism of FGF inhibition by SR1 differs from that of truncated transmembrane FGFR1. The mode of action of SR1 may be autocrine, paracrine, or endocrine, whereas that of truncated transmembrane FGFR1 is probably exclusively autocrine. But, as for SR1, complete inhibition of FGF activity was achieved only when the truncated transmembrane receptor was produced in large excess over the endogenous full-length FGFR.

In conclusion, the specific mode of SR1 generation, its specific localization relative to that of FGFR1, and

the specific kinetics of regulation of its mRNA, contrasting with the up-regulation of FGFR1 in activated RMG cells, strongly suggest a specific role for SR1 in normal and degenerating retina. This also suggests that SR1, as with other truncated soluble growth factor receptors, is not simple a consequence of the regulation of the level of the transmembrane receptor for a constant level of gene expression. The dramatic effects observed in the in vivo experiments of SR1 injected in the absence and presence of FGF2 in normal and degenerating retina highlight the significance of the generation of SR1 in normal and pathological conditions. We are currently studying the production of different FGF receptor type 1 forms by alternative splicing mechanisms in other retina degeneration models in which FGFs seem to be implicated.

ADDENDUM

While this paper was under review, another study addressing the inhibitory role of FGF soluble receptor 2 in multiorgan induction and patterning was published (Celli *et al*., 1998).

ACKNOWLEDGMENTS

We thank Dr. J.C. Jeanny for his expert technical assistance and his helpful suggestions. The excellent technical assistance of S. Thomasseau is gratefully acknowledged. We also gratefully acknowledge Dr. P. Caccia (Carlo-Erba Farmitalia, Neviana, Italy) for his generous contribution in providing human recombinant SR1. This work was supported by the Association pour la Recherche sur le Cancer and the Ministère de la Recherche et de l'Enseignement Supérieur.

REFERENCES

Baird, A., Esch, F., Gospodarowicz, D., and Guillemin, R. (1985). Retina and eye derived endothelial cell growth factors: partial molecular characterization and identity with acidic and basic fibroblast growth factor. Biochemistry *24*, 7855–7865.

Barnstable, J. (1991). Molecular aspects of development of mammalian optic cup and formation of retinal cell types. Prog. Retina Res. *10*, 45–69.

Beck, K.D. (1994). Functions of brain-derived neurotrophic factor, insulin-like growth factor-I and basic fibroblast growth factor in the development and maintenance of dopaminergic neurons. Prog. Neurobiol. *44*, 497–516.

Bergonzoni, L., Caccia, P., Cletini, O., Sarmientos, P., and Isacchi, A. (1992). Characterization of a biologically active extracellular domain of fibroblast growth factor receptor 1 expressed in *Escherichia coli*. Eur. J. Biochem. *210*, 823–829.

Caccia, P., Cletini, O., Isacchi, A., Bergonzoni, L., and Orsini, G. (1993). Biochemical characterization of the molecular interaction between recombinant basic fibroblast growth factor and a recombinant soluble fibroblast growth factor receptor. Biochem. J. *294*, 639–644.

Celli, G., LaRochelle, W.J., Mackem, S., Sharp, R., and Merlino, G. (1998). Soluble dominant-negative receptor uncovers essential roles for fibroblast growth factors in multi-organ induction and patterning. EMBO J. *17*, 1642–1655

Chirgwin, J.M., Preyzila, A.E., McDonald, R., and Rutter, J. (1978). Isolation of biological active ribonucleic acid from sources enriched in ribonuclease. Biochemistry *18*, 5294–5299.

Courlier, F., Pontarotti, P., Roubin, G., Goldfarb, M., and Birnbaum, D. (1997). Of worm to men: an evolutionary perspective on the fibroblast growth factor (FGF) and FGF receptor families. J. Mol. Evol. *44*, 43–56.

Courty, J., Loret, C., Moenner, M., Chevallier, B., Lagente, O., Courtois, Y., and Barritault, D. (1985). Bovine retina contains three growth factor activities with different affinity to heparin. Eye-derived growth factor, I, II, III. Biochimie *67*, 265–269.

Craig, A.D., Crumley, G., Bellot, F., Kaplow, J.M., Searfoss, G., Ruta, M., Burgess, W.H., Jaye, M., and Schlessinger, J. (1990). Cloning and expression of distinct high-affinity receptors cross-reacting with acidic and basic fibroblast growth factors. EMBO J. *9*, 2685–2692.

Deng, C.X., Winshaw-Boris, A., Shen, M.M., Daugherty, C., Ornitz, D.M., and Leder, P. (1994). Murine FGFR1 is required for early postimplantation growth and axial organization. Genes Dev. *8*, 3045–3057.

Duan, D.S.R., Werner, S., and Williams, L.T. (1992). A naturally occurring secreted form of fibroblast growth factor (FGF) receptor 1 binds basic FGF in preference over acidic FGF. J. Biol. Chem. *26*, 16076–16080.

Ekström, P., Sanyal, S., Narfström, K., Chader, G.J., and van Veen, T. (1988). Accumulation of glial fibrillary acidic protein in Müller radial glia during retinal degeneration. Invest. Ophthalmol. Visual Sci. *29*, 1363–1371.

Estival, A., Monza, V., Miquel, K., Gaubert, F., Hollande, E., Korc, M., Vaysset, N., and Clemente, F. (1996). Differential regulation of fibroblast growth factor (FGF) receptor-1 mRNA and protein by two molecular forms of basic FGF. J. Biol. Chem. *271*, 5663–5670.

Faktorovich, E.G., Steinberg, R.H., Yasumura, D., Matthes, M.T., and LaVail, M.M. (1992). Basic fibroblast growth factor and local injury protect photoreceptors from light damage in the rat. J. Neurosci. *12*, 3554–3567.

Friesen, J., Verge, V.M., Fried, K., Risling, M., Persson, H., Trotter, J., Hokfelt, T., and Lindholm, D. (1993). Characterization of glial trkB receptors: differential response to injury in the central and peripheral nervous system. Proc. Natl. Acad. Sci. USA *90*, 4971–4975.

Gao, H., and Hollyfield, J.G. (1995). Basic fibroblast growth factor in retinal development: differential levels of bFGF expression and content in normal and retinal degeneration (rd) mutant mice. Dev. Biol. *169*, 168–184.

Gao, H., and Hollyfield, J.G. (1996). Basic fibroblast growth factor: increased gene expression in inherited and light-induced photoreceptor degeneration. Exp. Eye Res. *62*, 181–189.

Gavrieli, Y., Sherman, Y., and ben-Sasson, S.A. (1992). Identification of programmed cell death in situ via specific labeling of nuclear DNA fragmentation. J. Cell Biol. *119*, 493–501.

Givol, D., and Yayon, A. (1992). Complexity of FGF receptors: genetic basis for structural diversity and functional specificity. FASEB J. *6*, 3362–3369.

Goureau, O., Jeanny, J., Hartmann, M.P., and Courtois, Y. (1993). Protection against light-induced retinal degeneration by an inhibitor of NO synthase. Neurosci. Res. *5*, 233–236.

Guillonneau, X., Tassin, J., Bryckaert, M., Ricard-Regnier, F., Courtois, Y., and Mascarelli, F. (1996). In vitro changes in plasma membrane heparan sulfate proteoglycans and in perlecan expression participate in the regulation of FGF2 mitogenic activity. J. Cell. Physiol. *166*, 170–187.

Hanneken, A., and Baird, A. (1995). Soluble forms of the high-affinity fibroblast growth factor receptor in human vitreous fluid. Invest. Ophthalmol. Visual Sci. *36*, 1192–1196.

Hanneken, A., Maher, P.A., and Baird, A. (1995). High affinity immunoreactive FGF receptors in the extracellular matrix of vascular endothelial cells. Implications for the modulation of FGF-2. J. Cell Biol. 128, *6*, 1221–1228.

Hanneken, A., Wenbin, Y., Ling, N., and Baird, A. (1994). Identification of soluble forms of the fibroblast growth factor receptor in blood. Proc. Natl. Acad. Sci. USA *91*, 9170–9174.

Jaye, M., Schlessinger, J., and Dionne, C.A. (1992). Fibroblast growth factor tyrosine kinases: molecular analysis and signal transduction. Biochem. Biophys. Acta *2*, 185–199.

Johnson, D.E., Lu, J., Chen, H., Werner, S., and Williams, L.T. (1991). The human fibroblast growth factor receptor genes: a common structural arrangement underlies the mechanisms for generating receptor forms that differ in their third immunoglobulin domain. Mol. Cell. Biol. *11*, 4627–4634.

Johnston, C.L., Cox, H.C., Gomm, J.J., and Coombes, R.C. (1995). Fibroblast growth factor receptors localize in different cellular compartments. J. Biol. Chem. *270*, 30643–30650.

Lee, P.L., Johnson, D., Cousens, L., Fried, A., and Williams, L.T. (1989). Purification and complementary DNA cloning of a receptor for basic fibroblast growth factor. Science *245*, 57–60.

Levi, E., Fridman, R., Miao, H.Q., Ma, Y.S., Yayon, A., and Vlodavsky, I. (1996). Matrix metalloproteinase 2 releases active soluble ectodomain fibroblast growth factor receptor 1. Proc. Natl. Acad. Sci. USA *93*, 7069–7074.

Lewis, G.P., Erickson, P.A., Guérin, C.J., Anderson, D.H., and Fisher, S.K. (1992). Basic fibroblast growth factor: a potential regulator of proliferation and intermediate filament expression in the retina. J. Neurosci. *12*, 3968–3978.

Li, Y., Basilico, C., and Mansukhani, A. (1994). Cell transformation by fibroblast growth factors can be suppressed by truncated fibroblast growth factor receptors. Mol. Cell. Biol. *14*, 7660–7669.

Mascarelli, F., Fuhrmann, G., and Courtois, Y. (1993). aFGF binding to low and high affinity receptors induces both aFGF and aFGF receptors dimerization. Growth Factors *8*, 211–233.

Mascarelli, F., Raulais, D., and Courtois, Y. (1989). Fibroblast growth factor phosphorylation and receptors in rod outer segments. EMBO J. *8*, 2265–2272.

Mascarelli, F., Tassin, J., and Courtois, Y. (1992). Effect of FGFs on adult bovine Muller cells: proliferation, binding and internalization. Growth Factors *4*, 81–95.

McDewitt, D., Brahma, S., Courtois, Y., and Jeanny, J.C. (1997). Fibroblast growth factors and regeneration of the eye lens. Dev. Dyn. *208*, 220–226.

Moscatelli, D. (1987). High and low affinity binding sites for basic fibroblast growth factor on cultured cells: absence of a role for low affinity binding in the stimulation of plasminogen activator production by bovine capillary endothelial cells. J. Cell. Physiol. *131*, 123–130.

Partanen, J., Vainakka, S., Korhonen, J., Armstrong, E., and Alitalo, K. (1992). Diverse receptors for fibroblast growth factor. Prog. Growth Factor Res. *4*, 69–83.

Robinson, M., MacMillan-Crow, L., Thompson, J., and Overbeek, P. (1995a). Expression of a truncated FGF receptor results in defective lens development in transgenic mice. Development *121*, 3959–3967.

Robinson, M., Overbeek, P., Verran, D., Grizzle, W., Stockard, C., Friesel, R., Maciag, T., and Thompson, J. (1995b). Extracellular FGF1 acts as a lens differentiation factor in transgenic mice. Development *121*, 505–514.

Ruta, M., Howk, R., Ricca, G., Drohan, W., Zabelshansky, M., Laureys, G., Barton, D.E., Francke, U., Schlessinger, J., and Givol, D. (1988). A novel protein tyrosine kinase gene whose expression is modulated during endothelial cell differentiation. Oncogene *3*, 9–15.

Torriglia, A., and Blanquet, P.R. (1992). Purification of an active receptor for acidic and basic fibroblast growth factor from bovine retina. Biochim. Biophys. Acta *1137*, 215–224.

Ueno, H., Gunn, M., Dell, K., Tseng, A., Jr., and Williams, L. (1992). A truncated form of fibroblast growth factor receptor 1 inhibits signal transduction by multiple types of fibroblast growth factor receptor. J. Biol. Chem. *267*, 1470–1476.

Wang, J.K., Guangxia, G., and Goldfarb, M. (1994). Fibroblast growth factor receptors have different signaling and mitogenic potentials. Mol. Cell. Biol. *14*, 181–188.

Wen, R., Song, Y., Cheng, T., Matthes, M.T., Yasumura, D., LaVail, M.M., and Steinberg, R.H. (1995). Injury-induced upregulation of bFGF and CNTF mRNAs in the rat retina. J. Neurosci. *15*, 7377–7382.

Wenkateswaren, S., Blanckaert, V., and Schelling, M. (1992). Production of anti-fibroblast growth factor receptor monoclonal antibodies by in vitro immunization. Hybridoma *11*, 729–739.

Werner, S., Duan, D.S., de Vries, C., Peters, K.G., Johnson, D.E., and Williams, L.T. (1992). Differential splicing in the extracellular region of fibroblast growth factor receptor generates receptor variants with different ligand-binding specificities. Mol. Cell. Biol. *12*, 82–88.

Wiedlocha, A., Faines, P.O., Madshus, I.H., Sandvig, K., and Olsnes, S. (1994). Dual mode of signal transduction by externally added acidic fibroblast growth factor. Cell *76*, 1039–1051.

Yamaguchi, T., Harpal, K., Henkemeyer, M., and Rossant, J. (1994). FGFR1 is required for embryonic growth and mesodermal patterning during mouse gastrulation. Development *8*, 3032–3044.

Yayon, A.M., Klagsbrun, J.D., Leder, P., and Ornitz, D.M. (1991). Cell surface, heparin-like molecules are required for binding of basic fibroblast growth factor to its high affinity receptor. Cell *64*, 841–848.